Plant Physiology Preview. Published on May 8, 2008, as DOI:10.1104/pp.108.119917

Running Head: Characterization of the *navel negra* stay-green citrus mutant

* Corresponding Author: Manuel Talón

Address: Ctra Moncada-Naquera km 5, 46113 Moncada, Valencia, Spain

Telephone: +34-963 424000

Fax: +34-963 424001

E-mail: mtalon@ivia.es

Journal research area: System Biology, Molecular Biology and Gene Regulation

An evaluation of the basis and consequences of a stay-green mutation in the *navel negra* (*nan*) citrus mutant using transcriptomic and proteomic profiling and metabolite analysis

Enriqueta Alós[1], María Roca[2], Domingo José Iglesias[1], Maria Isabel Mínguez-Mosquera[2], Cynthia Maria Borges Damasceno[3], Theodore William Thannhauser[4], Jocelyn Kenneth Campbell Rose[3], Manuel Talón[1]* and Manuel Cercós[1]

[1]Instituto Valenciano de Investigaciones Agrarias. Centro de Genómica. Ctra. Moncada-Náquera Km 5, 46113 Moncada, Valencia, Spain; [2]Chemistry and Biochemistry Pigments Group, Food Biotechnology Department, Instituto de la Grasa, Consejo Superior de Investigaciones Científicas (CSIC), Sevilla, Spain; [3]Department of Plant Biology, Cornell University, Ithaca, NY 147853, USA; [4]USDA Plant Soils and Nutrition Laboratory, Tower Road, Cornell University, Ithaca, NY 14853 USA.

* Corresponding author

Footnotes

Financial Sources: EA was the recipient of an INIA predoctoral fellowship and DJI and MC of INIA-CCAA contracts. JKCR was supported by the National Science Foundation's Plant Genome Program (Award # DBI 0606595). This work was supported by the Spanish Ministerio de Ciencia y Tecnología through grants Nº AGL2003-08502-C04-01 and GEN2001-4885-C05-03 and Instituto Nacional de Investigaciones Agrarias through grants Nº RTA03-106, 04-013 and 05-247.

Present address:

E. Alós: Department of Cell and Developmental Biology, John Innes Centre, Norwich Research Park, Colney, Norwich, NR4 7UH, UK.

Corresponding Author: Manuel Talón

Address: Instituto Valenciano de Investigaciones Agrarias. Centro de Genómica. Ctra. Moncada-Náquera Km 5, 46113 Moncada, Valencia, Spain

Telephone: +34-963 424000

Fax: +34-963 424001

E-mail: mtalon@ivia.es

ABSTRACT

A *Citrus sinensis* spontaneous mutant, *navel negra* (*nan*), produces fruit with an abnormal brown colored flavedo during ripening. Analysis of pigment composition in the wild type (WT) and *nan* flavedo suggested that typical ripening-related chlorophyll (Chl) degradation, but not carotenoid biosynthesis, was impaired in the mutant, identifying *nan* as a Type C stay-green mutant. *nan* exhibited normal expression of Chl biosynthetic and catabolic genes and chlorophyllase activity, but no accumulation of dephytylated chlorophyll compounds during ripening, suggesting that the mutation is not related to a lesion in any of the principal enzymatic steps in Chl catabolism. Transcript profiling using a citrus microarray indicated that a citrus ortholog of a number of *SGR* (*stay green*) genes was expressed at substantially lower levels in *nan*, both prior to, and during, ripening. However, the pattern of catabolite accumulation and *SGR* sequence analysis suggested that the *nan* mutation is distinct from those in previously described stay-green mutants and is associated with an upstream regulatory step, rather than directly influencing a specific component of Chl catabolism. Transcriptomic and comparative proteomic profiling further indicated that the *nan* mutation resulted in the suppressed expression of numerous photosynthesis-related genes and in the induction of genes that are associated with oxidative stress. These data, in addition to metabolite analyses, suggest that *nan* fruit employ a number of molecular mechanisms to compensate for the elevated Chl levels and associated photooxidative stress.

INTRODUCTION

Chlorophyll (Chl) degradation is central to the degreening process that is commonly observed in senescing leaves and the ripening of many fruit, and it has been estimated that approximately 1.2 billion tons of Chl are degraded annually (Hendry et al., 1987). However, despite its importance, the basic steps of the Chl catabolic pathway have only recently been elucidated and a few of the associated genes identified (Hörtensteiner, 2006). The degradation of Chl to a colorless fluorescent intermediate (primary fluorescent chlorophyll catabolite, pFCC) involves four basic steps, which are apparently common to all plants (Fig. 1): chlorophyllase (CLH) dephytylates chlorophyll *a*, producing chlorophyllide *a*; an unknown metal chelating substance (MCS) removes Mg and produces pheophorbide *a*; finally, pheophorbide *a* oxygenase (PaO) and red chlorophyll catabolite reductase (RCCR) convert pheophorbide *a* to red chlorophyll catabolite (RCC) and then to pFCCs. The conversion of pheophorbide *a* to RCC has been proposed as the key regulatory step of this pathway, since there is evidence indicating that PaO is the only enzyme of this pathway that is induced during senescence (Thomas et al., 2002), in the form of increased transcript abundance (reviewed in Hörtensteiner, 2006). The subsequent reactions are species-specific and involve multiple structural modifications of the pFCCs, before they are converted into nonfluorescent chlorophyll catabolites (NCCs) and are finally stored in the vacuole (Hörtensteiner, 2006). Despite excellent progress in characterizing the primary catabolic events, remarkably little is yet known about the factors that regulate the overall rate and extent of Chl breakdown (Hörtensteiner, 2006).

In this regard, important insights are likely to be provided through the identification and characterization of various ‘stay-green’ mutants that exhibit unusual Chl retention during leaf senescence or fruit ripening (Thomas and Howarth, 2000). Those identified to date span a broad taxonomic range, including members of the Gramineae (*Triticum durum* Desf., Spano et al., 2003; *Festuca pratensis*, Thomas, 1987; *Oryza sativa*, Cha et al., 2002, Park et al., 2007, Jiang et al., 2007, Kusaba et al., 2007), *Arabidopsis thaliana* (Ren et al., 2007, Oh et al., 2003, 2004, Woo et al., 2001) and the Leguminosae (*Glycine max* L. Merr., Guiamét and Giannibelli, 1994, 1996, Luquez and Guiamét, 2002; *Phaseolus vulgaris*, Bachman et al., 1994; Ronning et al., 1991; *Pisum sativum*, Armstead et al, 2007, Sato et al., 2007). A stay-green mutant phenotype

has also been reported in tomato fruits (the *green flesh* mutant of *Solanum lycopersicum*; Cheung et al., 1993; Akhtar et al., 1999) and pepper (*chlorophyll retainer*, Efrati et al., 2005; Roca and Mínguez-Mosquera, 2006). The molecular bases of the stay-green phenotype were first characterized in a *F. pratensis* mutant line showing accumulation of both chlorophyll *a* and the dephytylated chlorophyll catabolites chlorophyllide *a* and pheophorbide *a* (Thomas et al., 2002). After genetic and biochemical analyses, it was concluded that the mutant was affected in either the PaO gene or a specific regulator of this gene. Although biochemical lesions in PaO have been reported for several stay-green mutants (Hörtensteiner, 2006), other types of mutations can also result in stay-green phenotypes, such as chlorophyll b reductase in the rice *nyc1* mutant (Kusaba et al., 2007) and genes involved in LHCPII proteolysis in the *ore9* (Woo et al., 2001) and *ore10* (Oh et al., 2003, 2004) Arabidopsis stay-green mutants. In addition, it has been shown that RNA interference mediated knock-down of a *G. max* senescence-associated receptor-like kinase (GmSARK) confers a stay-green phenotype (Li et al., 2006).

A clearer understanding of the genetic basis of the control of chlorophyll degradation has only recently resulted from cloning of stay-green (*SGR*) genes from a *Lolium*/*Festuca* introgression (Armstead et al., 2006), rice (Park et al., 2007; Jiang et al., 2007), pea (Sato et al., 2007), tomato and pepper (Barry et al., 2008). Although the biochemical function of SGR proteins is not known, they contain a predicted chloroplast transit peptide and at least one SGR has been shown to bind LHCPII (light-harvesting complex protein) *in vivo* (Park et al., 2007). Transcript analyses further indicate that *SGR* gene expression is closely associated with leaf senescence (Armstead et al., 2006; Hörtensteiner, 2006; Sato et al., 2007) and transgenic Arabidopsis plants, in which both *SGR1* and *SGR2* genes are suppressed, show a stay-green phenotype, as has been previously observed in rice (Park et al., 2007). Thus, while *SGR* genes appear to play an important role in one of the early steps of Chl catabolism, much remains to be learnt about their mechanism of action. In addition, several transgenic plant lines have been reported that show stay-green phenotypes, such as those induced by altered hormone status, including increased amounts of cytokinins (Smart et al., 1991; Gan and Amasino, 1995) or decreased ethylene production (John et al., 1995). Clearly, numerous factors remain to be discovered that are directly, or indirectly, important in regulating Chl breakdown and it is likely that some of these will be identified through characterizing additional stay-green mutations.

This paper describes a spontaneous stay-green mutant, *navel negra* (*nan*) from *Citrus sinensis* (cv. Washington Navel), whose fruit fail to degreen during ripening, although the synthesis of carotenoids is not disrupted. The color change in citrus fruits is particularly evident in the flavedo, the outer colored exocarp of the citrus fruit peel (Davies and Albrigo, 1994), and involves differentiation of chloroplasts to chromoplasts (Rodrigo et al., 2004; Iglesias et al., 2001) and the biosynthesis of carotenoids. While several studies have described aspects of the latter in citrus fruits (Kato et al., 2004; Rodrigo et al., 2004; Alós et al., 2006), relatively little has been reported about citrus Chl biochemistry, although it has been shown that chlorophyllase (*CHL*), which is constitutively expressed during natural fruit development (Jacob-Wilk et al., 1999), is the rate limiting step of chlorophyll degradation in citrus peel (Harpaz-Saad et al., 2007), and that pheophorbide a oxygenase (*PaO*) and geranylgeranyl reductase (*CHL P*) expression correlates with Chl degradation (Alós et al., 2006). We present here an analysis of the Chl metabolite profile and gene expression pattern in *nan* that is distinct from previously reported stay-green mutants, and that suggests that the mutation is likely associated with an upstream regulatory event, rather than a lesion in a specific step in Chl catabolism. We also describe the use of a citrus microarray and 2D-DIGE analysis to contrast the transcriptome and proteome, respectively, of the *nan* flavedo with that of wild type orange at pre-ripe and ripe stages, in order to gain insights into the consequences of a stay-green mutation on tissue and cellular physiology.

RESULTS

Total flavedo pigment content

A mutant was identified among a population of *Citrus sinensis* trees, whose fruit developed a dark brown external color upon ripening, rather than the characteristic orange of the wild type (Fig. 2A). This coloration was confined to the flavedo (Fig. 2B) and no other unusual phenotypes were observed in either the fruit, which were typically green at pre-ripe stages, or in vegetative tissues. In order to determine the molecular basis of the abnormal coloration, pigment levels in the flavedo of the mutant, termed *navel negra* (*nan*), were compared with those from wild type (WT) fruit at a range of developmental and ripening stages, spanning 120-275 days postanthesis (DPA). The WT and *nan* fruit showed no differences in the levels of total Chls or carotenoids at

the immature and mature green stages (120-180 DPA; Fig. 2C and D). The apparent Chl depletion in *nan* and WT prior to ripening (120 to 180 DPA; Fig. 2C) reflects a dilution effect due to cell expansion in the fruit peel (Bain, 1958), rather than Chl degradation, since the ratio of dry weight to fresh weight decreased from 0.30 to 0.14 in WT, and from 0.32 to 0.16 in *nan*, resulting in a slight increase in the total amount of Chl (694 ± 42 to 772 ± 32 μg g^{-1} dry weight in WT and 733 ± 122 to 752 ± 68 μg g^{-1} dry weight in *nan*). However, while the abundance of Chl decreased during ripening to barely detectable levels in WT fruit, this did not occur in *nan* and levels remained unchanged (Fig. 2C) after natural color break (224 DPA). Furthermore, although both varieties showed a characteristic increase in carotenoid levels during ripening, consistent with the development of an orange color, they were substantially higher in *nan* fruit and were approximately double those of the WT at the fully ripe stage (275 DPA; Fig. 2D).

Measurement of chlorophylls, derivatives and chlorophyllase activity

The levels of Chls and their derivatives in the flavedo of both varieties were analyzed by HPLC at 3 developmental stages: mature green (180 DPA), breaker (224 DPA) and ripe (248 DPA, Table I). The concentrations of Chl *a* (105-120 μg g^{-1} FW) and Chl *b* (17-23 μg g^{-1} FW) showed a typical dramatic decrease during ripening in WT (≤ 98%), but remained high in *nan*, with almost no Chl degradation. Moreover, Chl dephytylated compounds (chlorophyllides and pheophorbides), which typically accumulate in PaO-affected stay-green mutants during ripening, were not detected in either *nan* or WT flavedo at any stage (Table I; Supplemental Fig. S1). Both varieties had similarly low levels of OH-chlorophyll *a*, pheophytin *a* and OH-chlorophyll *b* (Table I), although the oxidized chlorophylls were always more abundant in *nan* fruit. Despite the lack of Chl degradation in *nan*, no major differences were detected in chlorophyllase (CLH) activity between WT and *nan* in mature green or breaker fruits, and indeed, CLH activity was significantly higher in ripe *nan* fruit (Table I).

Expression of genes involved in pigment biosynthesis and degradation

The expression levels of a selection of genes associated with pigment biosynthesis and catabolism were quantified by real time RT-PCR during fruit development and ripening in the

flavedo of WT and *nan* (Fig. 3). These included: *phytoene synthase* (*PSY*), the first committed step in the carotenoid biosynthesis pathway (Fraser et al., 2002); *geranylgeranyl reductase* (*CHL P*), a gene involved in the biosynthesis of the phytyl chain of Chls (Tanaka et al., 1999); and two Chl catabolic genes, *PaO* and *RCCR*. Expression of *PSY* increased rapidly in both WT and *nan* flavedo, although maximal expression in WT was seen at the breaker stage, after which *PSY* transcript abundance decreased, while expression continued to increase during ripening in *nan*, peaking at the ripe stage, before decreasing during over ripening. The expression patterns of the genes involved in Chl biosynthesis and degradation were similar in WT and *nan*, in terms of both relative abundance and changes during fruit development (Fig. 3B-D).

Effect of ethylene on pigment composition and gene expression

The plant hormone ethylene is known to promote Chl degradation in the citrus flavedo (García-Luis et al., 1986; Jacob-Wilk et al., 1999) and so this phenomenon was examined in the *nan* mutant to determine whether the mutant phenotype might be associated with ethylene insensitivity. To this end, mature green WT and *nan* fruits were treated with 10 µl L^{-1} ethylene for 72 h, then total Chl and carotenoid levels were assayed and *PaO*, *CHL P*, *PSY* and *CLH* expression analyzed in flavedo tissues (Fig. 4). As expected, the ethylene treatment induced a substantial decrease in total Chl concentration in the WT flavedo (approximately 50 µg g^{-1} FW, which represents almost half of the initial content), while no significant change was detected in the *nan* flavedo (Fig. 4A). However, the expression patterns of *PaO* and *CHL P*, *PSY* and *CLH* showed similar changes in both varieties in response to the ethylene treatment (Fig. 3B), indicating that *nan* is ethylene responsive, but that this response is upstream of, or independent from, the signalling pathway that induces Chl degradation. Furthermore, the treatment did not alter total carotenoid content (Fig. 4A), although *PSY* expression increased to the same degree in both varieties (Fig. 4B).

Comparative transcriptome profiling

In order to gain insight into the potential basis and consequences of the stay-green phenotype, a survey of transcript expression in WT and *nan* flavedo was made using a 7,000

element citrus cDNA microarray (Forment et al., 2005). Pairwise analyses of RNA extracts from WT and *nan* flavedo tissue at the mature green, breaker and ripe stages identified 11 distinct genes that were differentially expressed in all 3 stages, of which 5 could be annotated based on sequence homology tBLASTx searches against the NCBI non-redundant database (Table II). The only EST that showed down regulation in the *nan* flavedo at all 3 developmental stages was a predicted s*tay-green* (*SGR)* gene homolog, with the highest degree of similarity to an *SGR* gene from tomato (Table II). In the *nan* mutant, 3 other genes, annotated as a *miraculin-like protein 2*, a *secretory peroxidase* and a *guanyl-nucleotide exchange factor*, showed up-regulation at the green stage and subsequent down-regulation (Table II). In contrast, the expression level of a *cysteine protease* was lower during the green stage but greater at the breaker and ripe stages (Table II). No significant sequence homology was apparent for the other 6 ESTs (CX299753, CX306150, CX299918, CX299940, CX287589 and CX289503) and, other than CX289503 that was expressed at higher levels in *nan* at all three stages, they exhibited similar relative expression patterns, with elevated transcript levels in the mutant flavedo at the mature green stage but reduced expression at the breaker and ripe stages (data not shown).

Since mutations in the *SGR* gene are responsible for the phenotype of several stay-green mutants (Armstead et al., 2007; Sato et al., 2007;Park et al., 2007; Ren et al., 2007; Jiang et al., 2007), a 1.2 kb genomic region, including the promoter and coding region, of the citrus *SGR* gene was cloned from WT and *nan* genomic DNA, (Genbank accession AM922109), but differences were not observed. Furthermore, to determine whether a deletion in one or more copies of the *SGR* gene could be responsible for the *nan* phenotype, the relative gene dosage of *SGR* was assessed in WT and *nan* by real-time PCR using genomic DNA and again no difference was observed (data not shown).

In addition to the 11 genes that showed differences in transcript abundance at all three stages, a broader group of genes showed significantly different expression levels at one or two stages (Supplemental Table S1). The annotated functions of these genes, which are divided into several classes in Tables III and IV, and their collective expression patterns, suggest two key trends. Firstly, at the mature green stage, a range of genes encoding components of the photosynthetic machinery and ancillary proteins associated with photosynthesis (e.g. NADPH: protochlorophyllide oxidoreductase, chlorophyll a/b binding protein, subunits of photosystems I and II and RuBisCO subunit binding-protein) were expressed at substantially lower levels in *nan*.

Secondly, many genes associated with abiotic stress, and particularly responses to high light and oxidative stress, were upregulated in *nan* at both the mature green (Tables III) and ripe (Table IV) stages. These included genes involved in the synthesis of compounds that ameliorate the effects of oxidative stress and reactive oxygen species (ROS), such as phenylpropanoids, polyamines and carotenoids, and with the synthesis of jasmonic acid, salicylic acid and ethylene, which have well established connections with biotic and abiotic stress-mediated signaling. To further verify that the *nan* phenotype is associated with increased oxidative stress, the concentration of ascorbic acid, an antioxidant compound that accumulates in response to oxidative stress in many plant species (Mitler et al., 2004), including citrus (Iglesias et al., 2006), was measured in extracts from WT and *nan* ripe flavedo. As predicted, ascorbic acid levels in ripe fruit flavedo were significantly greater in *nan* than WT (0.43 ± 0.04 and 0.29 ± 0.02 mg g^{-1} fresh weight, respectively).

In addition to these defined functional categories, a diverse set of genes with previously reported associations with oxidative stress showed differential expression between the varieties (Tables III and IV). For all putative functional categories, where a link between the apparent Arabidopsis ortholog of the citrus gene on the microarray and oxidative stress has been described in the literature, the corresponding reference is cited in Tables III and IV.

To validate the microarray results, quantitative RT-PCR analyses were performed of genes that represented different general patterns of expression (Table II) at the mature green, breaker and ripe developmental stages. Specifically, these comprised representatives of genes that in the *nan* mutant either showed reduced expression at all 3 stages (*stay-green protein*), higher expression at the mature green stage and then reduced expression during ripening (*secretory peroxidase*) or reduced expression in mature green fruits and increased transcript levels in ripening fruit (*cysteine protease*). In all cases, the expression patterns (Fig. 5) were essentially identical to those obtained with the microarray.

2D-DIGE analysis of protein expression

In a parallel analysis, and to complement the microarray study, a comparative proteomic survey was performed of the WT and *nan* flavedo at the same 3 stages, using 2-D Difference Gel Electrophoresis (2-D DIGE; Rose et al., 2004). The gel comparisons revealed 13 protein spots

that were consistently differentially expressed between *nan* and WT in all replicate analyses (arrows in representative gels shown in Supplementary Fig. 2). Differentially expressed spots were defined as those with a volume ratio above or below the 2 fold S.D. threshold, based on the normalized model curve of the spot volume ratio data set. Subsequent analyses by LC-ESI-MS/MS, followed by an interrogation of the NCBI non-redundant Green Plant database with the mass spectra using the Mascot search engine, identified a subset of 11 proteins (corresponding to those labeled 1-11 in Supplementary Fig. 2) with high confidence identification and annotation (Table V). These comprised a manganese superoxide dismutase (MnSOD), a copper zinc superoxide dismutase (CuZnSOD), the ribulose 1,5-bisphosphate carboxylase (RuBisCO) large subunit (two spots), 2 heat shock proteins (HSPs 19 and 21), a lectin-related protein, a glycine-rich RNA binding protein, a copper chaperone, an early light induced protein (ELIP) and finally, a protein with unknown function (gi|8778393). At the mature green stage, the only proteins that were detected with reduced expression in *nan* were HSP21 and the putative glycine-rich protein. HSP21, a protein involved in the chloroplast to chromoplast transition of tomato fruits (Neta-Sharir et al., 2005), was consistently less abundant in all 3 stages (–5.5, –3 and –2.7 fold, at mature green, breaker and ripe stages, respectively). Conversely, the two superoxide dismutases and the copper chaperone protein were upregulated in *nan* at the mature green stage. The two spots of the RuBisCO large subunit and the lectin-related precursor were less abundant in *nan* at breaker and ripe stages, while ELIP and HSP19 were expressed at higher levels than WT during ripening (Table V). This was particularly noticeable with ELIP, which was on average expressed at 14 fold higher levels in *nan* at the ripe stage

The 2D-DIGE screens were further validated by Western analysis of protein extracts from the flavedo of WT and *nan* at all 3 stages with a RuBisCO antiserum. The immunoblot analysis indicated that the RuBisCO large subunit (LSU) and small subunit (SSU) were expressed at lower levels in *nan*, in agreement with the 2D-DIGE analysis, and that protein abundance declined during ripening (Figure 6 and Table V). It should be noted that cDNAs for the RuBisCO LSU were not represented on the citrus microarray, but those of the SSU were present and the array analysis indicated that expression was statistically lower in breaker fruit. However, data generated by similar analyses with RNA from the mature green and ripe stages did not reach the P-value threshold for a statistically significant comparison (Supplemental Table S1).

The 2D-DIGE data were compared with the microarray study in an attempt to identify targets that were common to both analyses. Most of the microarray elements corresponding to the 10 proteins (other than RuBisCO) found in the 2D-DIGE study either did not generate expression data with significant P value thresholds in the microarray analyses, or were not represented on the array. Thus, only two differentially expressed putative unigenes in the citrus chip matched a high confidence best hit from the proteomic analyses (Table V and Supplementary Fig. S2): a lectin-related protein and HSP 19 (HSP19). For the lectin-related protein, statistically significant data in the two surveys indicated repression in the *nan* mutant of both mRNA (Supplemental Table S1) and protein (Table V) at the ripe stage. However, for the HSP19, transcript abundance was lower in *nan* at the mature green stage (Supplemental Table S1) while protein levels appeared to be higher (Table V) at ripe stage.

Gene expression of early light-inducible protein (ELIP)

The transcript levels corresponding to early light-inducible protein (ELIP), the protein with the greatest difference in expression between WT and *nan* flavedo (Table V), were quantified in the two varieties by real-time RT-PCR (Figure 7). Expression of *ELIP* in WT was relatively low until the breaker stage (214 DA), when levels increased dramatically, before peaking at the ripe stage and declining thereafter. In contrast, *ELIP* mRNA levels increased earlier in *nan*, prior the breaker stage and similarly declined somewhat earlier than WT during ripening.

DISCUSSION

The most striking phenotype of the *nan* mutant, which resulted in its initial identification, is the unusual brown color of the flavedo in the ripe fruit (Fig. 2A). An evaluation of the flavedo pigment composition indicated that *nan* can be defined as a Type C stay-green variant (Thomas and Howarth, 2000), since Chl levels remained elevated during ripening, rather than showing a typical decrease, while other ripening-related processes, such as carotenoids synthesis, proceeded normally (Fig. 2A and Table I). The brown coloration of *nan* fruit thus reflects the cumulative accumulation of Chl and carotenoids. This is further evidenced by the observation that *PaO,*

RCCR and *CHL P* transcript levels remained relatively constant, or showed only a small decrease during this period (Fig. 3B-D).

Descriptions of stay-green mutants with a major reduction in PaO activity from a range of plants species consistently report the accumulation of dephytylated intermediates in the Chl catabolic pathway during senescence (Hörtensteiner et al., 2006), and specifically elevated levels of pheophorbide *a* (Vicentini et al., 1995; Thomas et al., 1996; Roca et al., 2004), while no such accumulation has been detected in corresponding wild type plants. These stay-green mutants are therefore impaired in particular steps in Chl degradation, rather than showing down-regulation of the entire pathway. To compare *nan* with the previously characterized stay-green mutants, and to determine whether there are similarly distinct defects in specific steps in Chl catabolism, we measured the levels of Chl, Chl dephytylated compounds and CLH activity in the flavedo of *nan* and WT (Table I). Neither contained detectable levels of chlorophyllides or pheophorbides, although oxidized Chl derivatives were present in both varieties. Relatively low levels of OH-chlorophyll *a* were measured at the mature green stage in WT and *nan*, but were only detected in the mutant at the ripe stage and OH-chlorophyll *b* was also only observed in ripe *nan* flavedo. The accumulation of such hydroxylated Chl derivatives has previously been noted in several stay-green mutants and has been attributed to non-specific oxidation resulting from the elevated Chl levels, although the exact mechanism leading to their production is unknown (Roca and Mínguez-Mosquera, 2006). The patterns of CLH activity (Table I) and *PaO* and *RCCR* gene expression (Fig. 2) were similar in both varieties and the patterns of expression of *PSY, CHL P* and *PaO* were in close agreement with similar studies of other citrus species (Alós et al., 2006).

The response of the *nan* mutant to ethylene was also evaluated, since this hormone regulates leaf senescence (Kao and Yang, 1983; Choe and Whang, 1986) and color change in many fruit species, including citrus, through the activation of Chl degradation (García-Luis et al., 1986; Trebitsh et al., 1993; Jacob-Wilk et al., 1999) and carotenoid biosynthesis (Young and Jahn, 1972; Eilati et al., 1975). The results indicated that rapid ethylene-induced Chl loss was impaired in the *nan* mutant (Fig. 4), as has been previously reported in tomato and soybean stay-green mutants (Akhtar et al., 1999; Guiamét and Giannibelli, 1994). However, *nan* is ethylene responsive, since ethylene-induced gene expression, including transcripts involved in Chl synthesis and degradation or carotenoid biosynthesis, was similar in both varieties. While *PSY*

expression was upregulated in *nan* and WT (Fig. 4B), the time course of the analysis was not sufficiently long to generate significant changes in carotenoid levels (Fig. 4A).

These data suggest that the *nan* mutation is not directly related to a single disruption in any of the principal established enzymatic steps (CLH, PaO and RCCR) of Chl catabolism and is thus distinct from previously reported stay-green mutants. This hypothesis was explored by profiling transcript expression in the flavedo of WT and *nan* at the mature green, breaker and ripe stages. It was reasoned that genes whose expression was disrupted throughout fruit ontogeny might be more directly related to the function of the *nan* mutation, while those that showed differential expression only at later ripening stages might reflect secondary effects. Therefore, particular attention was paid to identifying transcripts with significantly different expression levels at all 3 stages. Interestingly, of the 11 genes that matched this criterion, the only one that was consistently downregulated was an *SGR* homolog that appears to be orthologous to Arabidopsis *SGR1* (Table II). Cloning and sequencing of the citrus *SGR* gene revealed no differences between WT and *nan* and no difference in gene dosage was detected in the two varieties. Taken together, the lack of Chl catabolite accumulation and the suppressed expression of the citrus *SGR* gene suggest that the *nan* mutation is associated with an early regulatory step that modulates *SGR* expression, rather than directly exerting a downstream effect on a specific aspect of catabolism.

In addition to characterizing the potential basis of the *nan* mutation, comparative transcriptomic and proteomic profiling were performed to assess the consequences of a stay-green mutation on flavedo tissue physiology, and to provide insights into the metabolic pathways that are affected. To date the only reported attempt at a larger scale study of differential gene expression in a stay-green mutant focused on three genes (*RuBisCO activase*, *soluble starch synthase* and *glycine decarboxylase*), which were identified through differential display screen of a durum wheat stay-green mutant (Rampino et al., 2006). These genes, together with those for RuBisCO small subunit (*rbcS*) and chlorophyll a/b/ binding protein (*cab*), were expressed at higher levels, or underwent a slower decline in abundance during senescence in the mutant. In addition, a study of the stay-green *greenflesh* tomato mutant suggested that the expression of several photosynthesis-related transcripts, or their cognate proteins, underwent a slower decrease in abundance in senescing leaves of the mutant than the wild type (Akhtar et al., 1999). Global transcript expression was monitored in the flavedo of *nan* and WT fruit at the mature green and

ripe stages to identify genes that were up- or down-regulated in the mutant. Published Arabidopsis microarray data were then analyzed manually, or using tools such as Genevestigator (www.genevestigator.ethz.ch), to identify developmental processes or stimuli that similarly influence transcript accumulation of the Arabidopsis orthologs of the differentially expressed citrus clones. A similar procedure was followed using differentially expressed proteins (Table V).

One particularly clear trend that emerged from the analysis was that a broad set of photosynthesis-related genes and proteins were downregulated in *nan* at the mature green stage (Tables III and IV), a phenomenon that is closely associated with high light-induced stress (Rossel et al., 2002; Kimura et al., 2003). Plants can adjust the size of the light harvesting antenna complex under such conditions and it is thought that this occurs in order to reduce the production of ROS, which are generated under excess light conditions (Escoubas et al., 1995; Heddad and Adamska et al., 2000). Oxidative stress-inducing treatments have also been reported to trigger the down-regulation of photosynthesis-associated genes (Tosti et al., 2006); thus, there appears to be feedback between cellular redox status and oxidative stress that represses photosynthetic function. In addition, the proteomic analysis identified rbcL as one of the major proteins with lower abundance in *nan* (Figs. 5 and 6 and Table V), which differs from the results seen with a rice *sgr* mutant (Sato et al., 2007) and retention of RuBisCO in leaves of the tomato *greenflesh* mutant (Akhtar et al., 1999), but agrees with the previously observed reduced RuBisCO protein levels in a *P. vulgaris* stay-green mutant (Bachmann et al., 1994).

If photosynthetic capacity is insufficient under conditions of excess absorbed light, free Chl can generate ROS, that in turn can cause extensive oxidative damage to the thylakoid membrane (Barber and Anderson, 1992; Niyogi, 1999). Accordingly, a second pattern that emerged from the proteomic and transcriptomic profiling was the association of genes that were among the most substantially up- or down-regulated in *nan* with abiotic stress, and specifically with high light or oxidative stress (Supplemental Table S1, Tables III and IV). While it is not practical to describe all the relevant genes and biochemical or physiological processes here, examples are shown in Tables III and IV, together with an associated report in the literature linking the specific Arabidopsis ortholog with stress responses or senescence. The *nan* flavedo had elevated levels of transcripts or proteins associated with enzymatic mechanisms for scavenging ROS, such as superoxide dismutase (SOD), and the biosynthesis of phenylpropanoids, polyamines and

isoprenoids, which provide nonenzymatic antioxidative protection (Apel and Hirt, 2004; Jordan, 2002; Kuehn and Phillips, 2005). Furthermore, the elevated carotenoid levels, higher ascorbic acid content and higher levels of OH chlorophylls in *nan* after the breaker stage of ripening (Fig. 2) were likely a response to ROS, as previously reported (Bouvier et al., 1998; Mitler et al., 2004). Another set of pathways that showed apparent upregulation in *nan* were those leading to the synthesis of ethylene, jasmonic acid and salicylic acid (Table 3). While these hormones have a well established role in regulating defence-responses following microbial challenge, there is increasing evidence that they are involved in substantial cross-talk between biotic and abiotic stress pathways and ROS-triggered molecular events (Fujita et al., 2006).

The comparative proteomic analyses also provided insights into the diversity of processes that were influenced by the *nan* mutation and, importantly, they revealed different gene targets from the microarray analyses: the two approaches were therefore complementary. The only identified protein that was expressed at lower levels in all 3 stages (Table V) was HSP21, a heat shock protein with chaperone-like activity (Lee et al., 1997). Although its biochemical function in fruit has yet to be fully elucidated, this chloroplastic protein has proposed roles in protection of photosystem II from photooxidative stress and in the conversion of chloroplasts to chromoplasts during fruit ripening (Neta-Sharir et al., 2005). The reduced expressed of HSP21 in *nan* may therefore be associated with the abnormal levels of Chl or altered plastid ontogeny in the mutant, for example if it participates in the disassembly of thylakoid membrane proteins and binding to partially folded or denatured proteins (Sun et al., 2002).

In contrast, the protein that showed the most relatively elevated expression in *nan* (Table V) was highly homologous to early light-induced proteins (ELIPs), which are thought to play a photoprotective role. ELIPs are known to bind to Chl (Adamska et al., 1999) and are expressed during processes involving both thylakoid assembly (Adamska et al., 1993) and disassembly, (Bartels et al., 1992; Adamska et al., 1992; Adamska and Kloppstech, 1994; Bhalerao et al., 2003), including the chloroplast to chromoplast transition (Bruno and Wetzel, 2004). Their accumulation in the thylakoid also correlates closely with the production of ROS and light stress (Adamska et al., 1992; Adamska et al., 1993; Adamska and Kloppstech, 1994; Hutin et al., 2003), in parallel with the reduced expression of Cab genes/proteins (Montané and Kloppstech, 2000; Kimura et al., 2003), as was observed in *nan* (Table III). In the *nan* mutant, a distinct time lag occurred between elevated levels of ELIP transcripts, which were seen at 190 DPA, long

before color break or an equivalent increase in WT (Figure 7), and increased levels of ELIP protein, which were not seen until color break and ripening (Figure 5, Table V). However, a lack of correlation between changes in steady state levels of ELIP transcripts and proteins was also noted in studies in Arabidopsis (Heddad et al., 2006). A recent report describing an *ELIP* gene knockout in Arabidopsis suggested that it did not affect tolerance to photoinhibition and photooxidative stress (Rossini et al., 2006), although the authors acknowledged that the many potential compensatory responses complicates interpretation of their data. Overall, a large body of evidence, including the coordinated upregulation of ELIP mRNA and protein levels with those of a range of adaptations to oxidative stress, supports a role for ELIPs in protection against photooxidative damage.

In conclusion, the gene and protein expression profiling analyses and metabolite analyses reveal that the *nan* mutant shows numerous hallmarks of oxidative stress. Some of these are readily apparent, in the form of genes or proteins with a defined role in senescence, or in providing protection against ROS (Table 3). In other examples, no clear mechanistic relationship with a response to oxidative stress is apparent, even though there is precedence for an association based on previous microarray analyses, such as is the case with β-amylase (Rossel et al., 2002; Table III). It is notable that *nan* shows substantial changes in gene and protein expressions at the mature green stage, prior to the normal onset of Chl degradation or any detectable difference in Chl levels compared with WT. This observation, together with the metabolite data, suggests that *nan* represents a new class of stay-green mutant with a lesion in a regulatory pathway that is upstream of *SGR*, and that the mutant exhibits symptoms of oxidative stress prior to the onset of the normal degreening process.

MATERIALS AND METHODS

Plant material and ethylene treatments

Fruits of *Citrus sinensis* cv. Washington Navel (WT, wild type) and the *navel negra* (*nan*) stay green mutant (cv. Navel Negra) were harvested from trees at the Instituto Valenciano de Investigaciones Agrarias (Moncada, Valencia, Spain) and a commercial orchard (Montserrat, Valencia, Spain), respectively. Sampling dates were July 26 2004 (120 DPA [days post

anthesis]) and then 180 (mature green stage), 190, 214, 224 (breaker stage), 248 (ripe stage), 260 and 275 DPA. For ethylene treatments, fruits were harvested at 180 DPA, when high levels of Chl were present in the flavedo, treated with 10 μl L^{-1} ethylene at 20 ºC in a sealed chamber and samples were taken at 0 and 72 h. Flavedo tissue from all samples was frozen in liquid nitrogen, powdered and stored at -80 ºC until pigment analysis or RNA extractions. Aliquots of the frozen ground tissue were lyophilized prior to protein extraction.

Total chlorophyll and carotenoids extraction and quantification

Chls and carotenoids were extracted with methanol and chloroform as in Rodrigo et al., (2003). Chl *a*, *b* and total (*a*+*b*) chlorophyll contents were calculated as in Smith and Benitez (1955) after measuring the absorbances at 644 and 662 nm. The pigment ethereal solution was then dried and saponified using 6% (w/v) KOH:methanol. Carotenoids were subsequently reextracted with diethyl ether until the hypophase was colorless. An aliquot of this extract was used for total carotenoid content quantification by measuring the absorbance at 450 nm and using the extinction coefficient of β-carotene ($\varepsilon^{1\%}$ = 2500; Davies, 1976).

All steps were carried out on ice and under dim light to prevent photodegradation, isomerizations and structural changes in the carotenoids. At least three independent extractions were performed for each sample.

Chlorophyll and derivatives extraction and HPLC analysis

Chl and derivatives were extracted as in Mínguez-Mosquera and Garrido-Fernández (1989) and Chls, chlorophyll derivatives and xanthophylls were retained in the DMF (dimethyl formamide) phase and analyzed by HPLC. Chl *a* and *b* standards were purchased from Sigma (Barcelona, Spain). Chlorophyllide a was formed by enzymatic deesterification of Chl a (Mínguez-Mosquera et al., 1994). The C-13 epimer of Chl *a* was prepared by treatment with chloroform (Watanabe et al., 1984) and 13^2-OH-Chl *a* and *b* were obtained as in Laitalainen et al., (1990). All standards were purified by NP- and RP-TLC (Mínguez-Mosquera et al., 1991, Mínguez-Mosquera et al., 1993). The separation and quantification of Chl degradation products were carried out by HPLC (HP 1100 Hewlett-Packard LC fitted with a HP1100 automatic injector), using a stainless steel column (25 x 0.46 cm i.d.), packed with 5μm C_{18} Superior ODS-

2 (Teknokroma, Barcelona, Spain). Separation was performed using an elution gradient (2 mL min^{-1}) with the mobile phases: water:ion pair reagent:methanol (1:1:8, v/v/v) and methanol:acetone (1:1, v/v), as in Mínguez-Mosquera et al., (1991). Sequential detection was performed with a photodiode array detector at 650 nm for series *b* and 666 nm for series *a* compounds. Data were collected and processed with an LC HP ChemStation (Rev.A.05.04). Pigments were identified by co-chromatography with authentic samples and from their spectral characteristics. The on-line UV-Vis spectra were recorded from 350 to 800 nm with the photodiode array detector. At least three independent extractions were performed for each sample.

Chlorophyllase activity

The method was an adaptation of that used by Terpstra and Lambers (1983). Flavedo tissue (5-10 g) was homogenized with 20 volumes of acetone at –20ºC. The supernatant was removed by filtration and the residue was treated again with 8 volumes of acetone. This operation was repeated until the supernatant was colorless. Finally, the precipitate was collected by vacuum filtration and left to dry at ambient temperature (20-25ºC). From each gram of fruit approximately 0.15 g of acetone powder was obtained. Extraction of the enzyme was carried out according to Johnson-Flanagan and Thiagarajah (1990). The acetone powder (0.5g) was extracted with 15 mL of 5 mM sodium phosphate buffer (pH 7), containing 50 mM KCl and 0.24 % (w/v) Triton X-100.

After centrifugation, the supernatant was used as a crude enzyme extract. The substrate, chlorophyll *a*, was isolated from fresh spinach leaves by pigment extraction using acetone (Holden, 1976), followed by TLC separation following as in Mínguez-Mosquera and Garrido-Fernández (1989). The standard reaction mixture (1.1 mL) contained approximately 0.1 µmol of Chl *a* in acetone, 100mM Tris buffer (pH 8.5) containing 0.24% (w/v) Triton-X-100 and enzyme extract, in a 1:5:5 ratio. Chlorophyllide *a* levels were quantified as described by Mínguez-Mosquera et al., (1994) and the results are expressed as µmol h^{-1} g^{-1} FW. At least three independent extractions were performed for each sample.

Ascorbic acid quantification

Disks of flavedo tissue were excised, frozen in liquid nitrogen, ground to a fine powder and 500 mg of each sample was homogenized in 5 ml of 2 % metaphosphoric acid. After centrifugation (5000g, 4ºC, 10 min) and filtration, the ascorbic acid contect of the supernatant was spectrophotometrically measured (as described by Takahama and Oniki, 1992) with a Cary 50 Bio spectrophotometer (Varian Inc., USA). Concentration was determined monitoring the absorbance decrease at 265 nm due to the oxidation of ascorbate to deydroascorbate, catalyzed by ascorbate oxidase (EC 1.10.3.3., from *Cucurbita* spp.). At least, three independent determinations per sample were performed.

RNA extraction and real time RT-PCR

Total RNA was isolated from frozen flavedo using the RNeasy Plant Mini Kit (Qiagen, Madrid, Spain) and treated with RNase-free DNase (Qiagen) according to the manufacturer's instructions. UV absorption spectrophotometry and agarose gel electrophoresis were performed to test RNA quality as described by Sambrook et al., (1989). Quantitative real-time RT-PCR was performed with a LightCycler 2.0 Instrument (Roche, Barcelona, Spain) equipped with LightCycler Software version 4.0 (Roche) as described in Alós et al., (2006). Specificity of the amplification reactions was assessed by post-amplification dissociation curves and by sequencing the reaction products. To transform fluorescent intensity measurements into relative mRNA levels, a ten-fold dilution series of a RNA sample was used as standard curve. Reproducible data were obtained after normalization to total RNA amounts accurately quantified with the RNA-specific fluorescent dye Ribogreen (Molecular Probes, OR, USA; Bustin, 2002; Hashimoto et al., 2004). Each sample was analyzed in triplicate and means ± S.E. were calculated. Induction values of 1-fold were arbitrarily assigned to the 120 DPA sample for the natural ripening associated gene expression. In the ethylene treatment experiment, the expression ratio between the treated and untreated fruits was calculated and log-transformed. To validate the microarray data, real time PCR of three selected genes was performed in triplicate and expression levels log-transformed. The sequences of the primers used for the real-time RT-PCR and associated references that were used for primer design are shown in Supplemental Table S2.

Genomic DNA extraction and real-time PCR

Genomic DNA was isolated from frozen leaves using the DNeasy Plant Mini Kit (Qiagen) according to the manufacturer's instructions. UV absorption spectrophotometry and agarose gel electrophoresis were performed to test RNA quality as described by Sambrook et al., (1989). DNA concentration was accurately quantified with the DNA-specific fluorescent dye Picogreen (Molecular Probes, OR, USA).

To determine the relative gene dosage of *SGR* in WT and *nan* by quantitative real-time PCR two specific oligonucleotide primers, sgrZCF (5'-AGTTTGGTTGCTGCTCTTGG-3') and sgrZCR (5'-AGTGCGTTTTGCTGCTCATA-3'), were designed corresponding to positions 93-112 and 160-141, respectively, in the 566 bp *SGR* cDNA insert (accession number CX308230). PCR was carried out with 1 ng genomic DNA adding 2 µl LC FastStart DNA MasterPLUS SYBR Green I (Roche) and 2.5 pmol of each primer in a total volume of 10 µl. Incubations were carried out at 95 ºC 10 min followed by 40 cycles at 95 ºC 2 seconds, 55 ºC 10 seconds and 72 ºC 15 seconds. Fluorescent intensity data were acquired during the 72 ºC extension step. Specificity of the amplification reactions was assesed by post-amplification dissociation curves and by sequencing the reaction products. To transform fluorescent intensity measurements into relative DNA levels, a ten-fold dilution series of a DNA sample was used as standard curve. Each sample was analyzed in triplicate and means ± S.E. were calculated.

Cloning and sequencing the SGR genomic region

The promoter region of the citrus *SGR* gene was cloned from WT genomic DNA using the GenomeWalker Universal Kit (Clontech) following the manufacturer's instructions, except that six GenomeWalker libraries were constructed using the restriction enzymes *Dra*I, *Eco*RV, *Hinc*II, *Pvu*II, *Sca*I and *Sma*I. Two gene-specific oligonucleotide primers, sgrA (5'-CTCTGACTGAGTGGGAGAG-3') and sgrB (5'-GTTGAAACGACCTGAC-3'), were designed corresponding to positions 66-48 and 31-16, respectively, in the 5' end of the 566 bp *SGR* cDNA insert (accession number CX308230). After two nested PCR reactions, a single 800 bp product was amplified from the *Dra*I library, cloned into the pCR2.1 vector (Invitrogen) and fully sequenced from both ends.

The genomic region containing the promoter and coding region of the *SGR* gene was cloned by PCR using genomic DNA from both *nan* and WT using a forward primer specific for the 5' end of the promoter region (sgrF: 5'-CTGACTCCCAGCGCAATTAC-3') and a reverse primer specific for the 3' end of the cDNA, adjacent to the poly-A tail (sgrR: 5'-TCAAGATTCCATCTCAAAAGCTC-3'). The PCR reaction mix consisted of 5 ng genomic DNA, 1 µl 10 mM dNTP mix, 5 pmol of each oligonucleotide, 2.5 µl 10X reaction buffer and 0.5 µl Advantage 2 polymerase mix (Clontech). Touch-down PCR was carried out under the following conditions: 5 min at 95 ºC, 10 cycles of 30 seconds at 95 ºC, 1 min at the annealing temperature, decreasing 1 ºC per cycle from 65 ºC to 55 ºC and 3 min at 72 ºC, then 35 cycles of 30 seconds at 95 ºC, 1 min at 55 ºC and 3 min at 72 ºC and a final extension step at 72 ºC for 5 min. A single band of 1.2 kb was amplified from each of the genomic DNA samples. The products were cloned into the pCR2.1 vector and plasmid DNA from 12 independent clones of each product was fully sequenced from both ends.

Microarray hybridisation and analysis

Sample labeling, microarray hybridization and washing and data acquisition and analysis were performed as described in Cercós et al., (2006) RNA was extracted from each sample, with at least three biological replicates and independently processed, labeled and hybridized to different microarrays. Differences in gene expression were considered to be significant when a P-value was <0.001 and the induction or repression ratio was equal or higher than 2-fold. Only high quality PCR spots (Forment et al., 2005) were used for analyses.

2D-DIGE analysis

Proteins were extracted from WT and *nan* flavedo tissue of mature green (180 DPA), breaker (224 DPA) and ripe (248 DPA) fruits as in Saravanan and Rose (2004). Protein concentrations were quantified with the BioRad protein assay (BioRad, CA, USA) using BSA as a standard. Protein labeling (50 µg per extract) was performed using Cy Dye DIGE fluors (Amersham Biosciences, NJ, USA) according to the manufacturer's instructions. IPG strips (24 cm, linear pH 4-7, BioRad ReadyStrip; BioRad) were rehydrated overnight with 450 µL IEF buffer containing the Cy Dye-labeled protein mixture described above and focused using a Protean IEF Cell

(BioRad) at 20 ºC. The following program was applied: a linear increase from 0 to 500 V over 1 h, 500 V to 10^4 V over 5 h and then held at 10^4 V for a total of 100 kVh. After focusing, the proteins were reduced by incubating the IPG strips with 2 % (w/v) DTT for 10 min and alkylated with 2 % (w/v) iodoacetamide in 10 mL of equilibration buffer (6M urea, 20 % (v/v) glycerol, 3 % (w/v) SDS and 375 mM Tris-HCl pH 8.8) for 10 min. The strips were then transferred to 12.5 % SDS-PAGE gels for second dimension electrophoresis with the Ettan Dalt six gel system (Amersham Biosciences), using SDS electrophoresis buffer (25 mM Tris, 192 mM glycine, 0.1% (w/v) SDS) with 2 W per gel for 16 h. Four independent extracts were made from each sample, resulting in 4 replicate gels for each developmental stage. In each comparison, WT samples were labeled with the Cy3 dye in three gels and a dye-swap was performed in the fourth.

Cy3 and Cy5 images were collected using a Typhoon scanner (Amersham Biosciences) in fluorescence mode at 100 μm resolution. Images were analyzed using ImageQuant version 5.2 (Amersham Biosciences) and Decyder version 4.0 (Amersham Biosciences). Spot volumes were determined after background subtraction and volume ratio values were normalized, so that the modal peak of volume ratios was zero. Differentially expressed spots were defined as those with a volume ratio above or below the 2 S.D. threshold. Final spot ratio values are means ± S.E. of four independent biological replicates for each developmental stage.

Protein identification

Gels were fixed in water:methanol:acetic acid (83:10:7, v/v/v) for 2 h and subsequently stained with colloidal Coomassie G-250. Gel plugs containing protein spots of interest were manually excised, washed with 50 μL of water for 5 min and 50 μL of acetonitrile (ACN):50 mM, ammonium bicarbonate (ABC, 1:1, v/v) for 10 min, rehydrated in 15 μL trypsin solution (10 ng/μL in 25 mM ABC) and covered with 10 μL of 50 mM ABC. After overnight incubation at 37 ºC, the supernatant was collected and peptides were reextracted sequentially with 60 μL of acetonitrile:formic acid (20:1, v/v) and 30 μL of acetonitrile:formic acid (180:1, v/v). The supernatants were combined and dried in a speed-vac (ThermoSavant, MA, USA).

The samples were reconstituted in 10 μL of 0.1% formic acid/2% acetonitrile (v/v) for LC-ESI-MS/MS analysis. The CapLC was carried out with an LC Packings Ultimate integrated capillary HPLC system equipped with a Switchos valve switching unit (Dionex, CA, USA). The

gel-extracted peptides (6.4 µL) were injected using a Famous autosampler (Dionex) onto a C18 µ-precolumn cartridge (5 µm, 300 µm × 5 mm, Dionex) for on-line desalting, and then separated on a PepMap C-18 RP capillary column (3 µm, 300 µm id × 150 mm, Dionex). Peptides were eluted in a 30-minute gradient of 5% to 45% acetonitrile in 0.1% formic acid at 4 µL min^{-1}. The CapLC was connected in-line to a hybrid triple-quadrupole linear ion trap mass spectrometer, 4000 Q Trap (ABI/MDS Sciex, Framingham, MA) equipped with a Turbo V source. Data acquisition was performed using Analyst 1.4 software (Applied Biosystems) in the positive ion mode for information dependant acquisition (IDA) analysis. In an IDA analysis, after each survey scan from *m/z* 400 to *m/z* 1600, an enhanced resolution scan was performed followed by MS/MS of the three highest intensity ions with multiple charge states. The MS/MS data were submitted to Mascot 1.9 for a database search against the NCBI non-redundant green plant database. The search was performed allowing one trypsin miscleavage site and the peptide tolerance and MS/MS tolerance values were set to 0.8 Da and 2 Da, respectively. Only significant scores defined by a Mascot probability analysis (www.matrixscience.com/help/scoring_help.html#PBM) greater than "identity" were considered for assigning protein identity.

Immunoblot analysis

Immunoblot analysis was carried with the same flavedo tissue samples used for the 2D-DIGE experiments. Ground flavedo tissue (500 mg) was resuspended in 2 mL of 50 mM Tris-HCl pH 7.5 and 20 µL 100 mM PMSF, incubated for 30 min at 2 ºC and centrifuged at 10^4 *g* at 4 ºC. The supernatant was collected and quantified by the Bradford assay (see above). Protein extracts (5 µg per lane) were separated by SDS-PAGE on 12.5% polyacrylamide gels (BioRad). Gels were stained with SyproRuby (BioRad), to confirm equivalent sample loading, or transferred to Hybond ECL membranes, according to the manufacturer's instructions (Amersham Life Science, Cleveland, USA). Immunoblot analysis was performed after blocking the membranes in 3% (w/v) bovine serum albumin and 0.02% (w/v) sodium azide in sterile PBS-Tween (1x PBS/ 0.1% (v/v) Tween 20), using the ECL Western-blotting kit, according to the manufacturer's instructions (Amersham Life Science). The blot was incubated with RuBisCO antiserum (diluted $1:10^4$ in PBS-Tween) followed by a $1:2 \times 10^4$ dilution of the horseradish peroxidase-conjugated

secondary antibody. After each incubation with antiserum, the membrane was washed three times in PBS-Tween.

Supplemental material

The following materials are available in the online version of this article:

Supplemental Table S1. Microarray results of genes that showed statistically significant differences in expression levels between navel negra (*nan*) flavedo versus Washington Navel wild type (WT) flavedo at the mature green and ripe stages.

Supplemental Table S2. Oligonucleotides used as primers for real-time RT-PCR.

Supplemental Figure S1. HPLC chromatograms of chlorophylls and derivatives in WT and *nan* ripe fruit.

Supplemental Figure S2. Overlay images from 2-D DIGE analysis.

All the microarray data described in this study were deposited into the ArrayExpress database (accession no. E-MEXP-967). The sequence described in this study was deposited into GenBank database (accession no. AM922109).

ACKNOWLEDGMENTS

We acknowledge Isabel Sanchis, Israel Morte, and Angel Boix for technical support and thank Tal Isaacson and Eric Schaffler their help with 2D gel Analysis.

LITERATURE CITED

Adamska I, Ohad I, Kloppstech K (1992) Synthesis of the early light-inducible protein is controlled by blue light and related to light stress. Proc Natl Acad Sci USA **89**: 2610-2613

Adamska I, Kloppstech K, Ohad I (1993) Early light-inducible protein in pea is stable during light stress but is degraded during recovery at low light intensity. J Biol Chem **268**: 5438-44

Adamska I, Kloppstech K (1994) Low temperature increases the abundance of early light-inducible transcript under light stress conditions. 1994. J Biol Chem **269**: 30221-30226

Adamska I, Roobol-Bóza M, Lindahl M, Andersson B (1999) Isolation of pigment-binding early light-inducible proteins from pea. Eur J Biochem **260**: 453-460

Akhtar MS, Goldschmidt EE, John I, Rodoni S, Matile P, Grierson D (1999) Altered patterns of senescence and ripening in gf, a *stay-green* mutant of tomato (*Lycopersicon esculentum* Mill.). J Exp Bot **336**: 1115-1122

Apel K and Hirt H (2004) Reactive oxygen species: metabolism, oxidative tress and signal transduction. Ann Rev Plant Biol **55**: 373-399

Alós E, Cercós M, Rodrigo MJ, Zacarías L, Talón M (2006) Regulation of color break in Citrus fruits. Changes in pigment profiling and gene expression induced by gibberellins and nitrate, two ripening retardants. J Agric Food Chem **54**: 4888-4895

Armstead I, Donnison I, Aubry S, Harper J, Hörtensteiner S, James C, Mani, J, Moffet M, Ougham H, Roberts L, Thomas A, Weeden N, Thomas H, King I (2006) From crop to model to crop: identifying the genetic basis of the stay-green mutation in the *Lolium*/*Festuca* forage and amenity grasses. New Phytol **172**: 592-597

Armstead I, Donnison I, Aubry S, Harper J, Hörtensteiner S, James C, Mani, J, Moffet M, Ougham H, Roberts L, Thomas A, Weeden N, Thomas H, King I (2007) Cross-species identification of Mendel's *I* locus. Science **315**: 73.

Bachmann A, Fernández-López J, Ginsburg S, Thomas H, Bouwkamp JC, Solomos T, Matile P (1994) Stay-green genotypes of *Phaseolus vulgaris* L.: chloroplast proteins and chlorophyll catabolites during foliar senescence. New Phytol **126**: 593-600

Bain JM (1958) Morphological, anatomical and physiological changes in the developing fruit of the Valencia orange *Citrus sinensis* (L) Osbeck. Aust J Bot **6**: 1-24

Barber J, Andersson B (1992) Too much of a good thing: light can be bad for photosynthesis. Trends Biochem Sci **17**: 61-66.

Barry CS, McQuinn RP, Chung M-Y, Besuden A, Giovannoni JJ (2008) Amino acid substitutions in homologs of the STAY-GREEN (SGR) protein are responsible for the *green-flesh* and *chlorophyll retainer* mutations of tomato and pepper. Plant Physiol. Published online March 21, 2008; 10.1104/pp.108.118430

Bartels D, Hanke C, Schneider K, Michel D, Salamini F (1992) A desiccation-related ELIP-like gene from the resurrection plant *Crateostigma plantagineum* is regulated by light and ABA. EMBO **11**: 2771-2778

Bhalerao R, Keskitalo J, Sterky F, Erlandsson R, Björkbacka H, Birve SJ, Karlsson J, Gardeström P, Gustafsson P, Lundeberg J, Jansson S (2003) Gene expression in autumn leaves. Plant Physiol. **131**: 430-442

Bouvier F, Backaus RA, Camara B (1998) Induction and control of chromoplast-specific carotenoid genes by oxidative stress. J Biol Chem **273**:30651-30659

Bray EA (2002) Classification of genes differentially expressed during water-deficit stress in *Arabidopsis thaliana*: an analysis using microarray and differential expression data. Annal Bot **89**: 803-811

Bruno AK, Wetzel CM (2004) The early light-inducible protein (ELIP) gene is expressed during chloroplast-to chromoplast transition in ripening tomato fruit. J Exp Bot **408**:2541-2548

Bustin SA (2002) Quantification of mRNA using real-time reverse transcription PCR (RT-PCR): trends and problems. J Mol Endocrin **29**: 23-39

Cercós M, Soler G, Iglesias DJ, Gadea J, Forment J, Talón M (2006) Global analysis of gene expression during development and ripening of Citrus fruit flesh. A proposed mechanism for citric acid utilization. Plant Mol Biol **62**: 513-527

Cha KW, Lee YJ, Koh HJ, Lee BM, Nam YW, Paek NC (2002) Isolation, characterization, and mapping of the stay green mutant in rice. Theor Appl Genet **104**: 526-532

Chen F, D'Auria JC, Tholl D, Ross JR, Gershenzon J, Noel JP, Pichersky E (2003) An *Arabidopsis thaliana* gene for methylsalicylate biosynthesis, identified by a biochemical genomics approach, has a role in defense. Plant J **36**: 577-588

Cheung AY, McNellis T, Piekos B (1993) Maintenance of chloroplast components during chromoplast differentiation in the tomato mutant green flesh. Plant Physiol **101**: 1223-1229

Choe HC, Whang M (1986) Effects of ethephon on aging and photosynthetic activity in isolated chloroplasts. Plant Physiol **80**: 305-309

Davies BH (1976) Carotenoids. In Chemistry and Biochemistry of plant pigments, TW Goodwin, ed. Academic Press, New York, pp 38-165

Davies FS, Albrigo LG (1994) Citrus. CAB International, Oxon, pp 202-215

de la Torre F, De Santis L, Suárez MF, Crespillo R, Cánovas FM (2006) Identification and functional analysis of a prokaryotic-type aspartate aminotransferase: implications for plant amino acid metabolism. Plant J **46**: 414-425

Debnam PM, Fernie AR, Leisse A, Golding A, Bowsher CG, Grimshaw C, Knight JS, Emes MJ (2004) Altered activity of the P2 isoform of plastidic glucose 6-phosphate dehydrogenase in tobacco (*Nicotiana tabacum* cv. Samsun) causes changes in carbohydrate metabolism and response to oxidative stress in leaves. Plant J **38**: 49-59

Efrati A, Eyal Y, Paran I (2005) Molecular mapping of the chlorophyll retainer (cl) mutation in pepper (*Capsicum spp*.) and screening for candidate genes using tomato ESTs homologous to structural genes of the chlorophyll catabolism pathway. Genome **48**: 347-351

Eilati SK, Budowski P, Monselise SP (1975) Carotenoid changes in the Shamouti orange peel during chloroplast-chromoplast transformation on and off the tree. J Exp Bot **26**: 624-632

Escoubas JM, Lomas M, Laroche J, Falkowski PG (1995) Light-intensity regulation of Cab gene transcription is signaled by the redox state of the plastoquinone pool. Proc Natl Acad Sci USA **92**: 10237-10241

Forment J, Gadea J, Huerta L, Abizanda L, Agustí J, Alamar S, Alós E, Andrés F, Arribas R, Beltrán JP, Berbell A, Blázquez MA, Brumós J, Cañas, LA, Cercós M, Colmenero-Flores JM, Conesa A, Estables, B, Gandía M, García-Martínez JL, Gimeno J, Gisbert A, Gómez G, González-Candelas L, Granell, A, Guerri, J, Lafuente, MT, Madueño F, Marcos JF, Marqués MC, Martínez F, Martínez-Godoy MA, Miralles S, Moreno P, Navarro L, Pallás V, Pérez-Amador MA, Pérez-Valle J, Pons C, Rodrigo I, Rodríguez PL, Royo C, Serrano R, Soler G, Tadeo F, Talón M, Terol J, Trenor M, Vaello L, Vicente O, Vidal C, Zacarías L, Conejero V (2005) Development of a citrus genome-wide

EST collection and cDNA microarray as resources for genomic studies. Plant Mol Biol **57**: 375-391

Fraser PD, Romer S, Shipton CA, Mills PB, Kiano JW, Misawa N, Drake RG, Schuch W, Bramley PM (2002) Evaluation of transgenic tomato plants expressing an additional phytoene synthase in a fruit-specific manner. Proc Natl Acad Sci USA **99**:1092-1097

Fujita M, Fujita Y, Noutoshi Y, Takahashi F, Narusaka Y, Yamaguchi-Shinozaki K, Shinozaki K (2006) Crosstalk between abiotic and biotic stress responses: a current view from the points of convergence in the stress signaling networks. Curr Opin Plant Biol **9**: 436-442

Gadjev I, Vanderauwera S, Gechev TS, Laloi C, Minkov IN, Shulaev V, Apel K, Inzé D, Mittler R, Van Breusegem F (2006) Transcriptomic footprints disclose specificity of reactive oxygen species signaling in Arabidopsis. Plant Physiol **141**: 436-445

Gan S, Amasino RM (1995) Inhibition of leaf senescence by autoregulated production of cytokinin. Science **270**: 1986-1988

García-Luis A, Fornes F, Guardiola JL (1986) Effects of gibberellin A_3 and cytokinins on natural post-harvest, ethylene-induced pigmentation of Satsuma mandarin peel. Physiol Plant **68**: 271-274

Gepstein S, Sabehi G, Carp M-J, Hajouj T, Nesher MFO, Yariv I, Dor C, Bassani M (2003) Large-scale identification of leaf senescence-associated genes. Plant J **36**: 629-642

Guiamét, JJ Giannibelli MC (1994) Inhibition of the degradation of chloroplast membranes during senescence in nuclear 'stay green' mutants of soybean. Physiol Plant **91**: 395-402

Guiamét JJ, Giannibelli MC (1996) Nuclear and cytoplasmic 'stay-green' mutations of soybean alter the loss of leaf soluble proteins during senescence. Physiol Plant **96**: 655-661

Guo Y, **Cai Z**, **Gan S** (2004). Transcriptome of *Arabidopsis* leaf senescence. Plant Cell Environ **27**: 521–549

Harpaz-Saad S, Azoulay T, Arazi T, Ben-Yaakov E, Mett A, Shiboleth YM, Hörtensteiner S, Gidoni D, Gal-On A, Goldschmidt, EE, Eyal Y (2007) Chlorophyllase is a rate-limiting enzyme in chlorophyll catabolism and is posttranslationally regulated Plant Cell **19**: 1007-1022

Hashimoto JG, Beadles-Bohling AS, Wiren KM (2004) Comparison of RiboGreen and 18S rRNA quantitation for normalizing real-time RT-PCR expression analysis. BioTech **36**: 54-60

Heddad M, Adamska I (2000) Light stress-regulated two-helix proteins in Arabidopsis thaliana related to the chlorophyll a/b binding gene family. Proc. Natl. Acad. Sci. USA **97**: 3741-3746

Heddad M, Norén H, Reisewr V, Dunaeva M, Andersson B, Adamska I (2006) Differential expression and localization of early light-induced proteins in Arabidopsis. Plant Physiol **142**: 75-87

Hendry GAF, Houghton JD, Brown SB (1987) The degradation of chlorophyll. A biological enigma. New Phytol **107**: 255-302

Holden M (1976) Analytical methods chlorophylls. In: Chemistry and Biochemistry of Plant Pigments. T.W. Goodwin, ed. Academic Press, London, Vol. II, pp 1-37

Hörtensteiner S (2006) Chlorophyll degradation during senescence. Annu Rev Plant Biol **57**: 55-77

Hutin C, Nussaume L, Moise N, Moya I, Kloppstech K, Havaux M (2003) Early light-induced proteins protect Arabidopsis from photooxidative stress. Proc Natl Acad Sci USA **100**:4921-4926

Iglesias DJ, Tadeo FR, Legaz F, Primo-Millo E, Talon M (2001) In vivo sucrose stimulation of colour change in citrus fruits epicarps: Interactions between nutritional and hormonal signals. Physiol Plant **112**: 244-250

Iglesias DJ, Calatayud A, Barreno E, Primo-Millo E, Talon M (2006) Responses of citrus plants to ozone: leaf biochemistry, antioxidant mechanisms and lipid peroxidation. Plant Physiol Biochem **44**: 125-131.

Inada S, Ohgishi M, Mayama T, Okada K, Sakai T (2004) RPT2 is a signal transducer involved in phototropic response and stomatal opening by association with phototropin 1 in *Arabidopsis thaliana*. Plant Cell **16**: 887-896

Jacob-Wilk D, Holland D, Goldschmidt EE, Riov J, Eyal Y (1999) Chlorophyll breakdown by chlorophyllase: isolation and functional expression of the Chlase1 gene from ethylene-treated Citrus fruit and its regulation during development. Plant J **20**: 653-661

Jiang H, Li M, Ling N, Yan H, Xu X, Liu J, Xu Z, Chen F, Wu G (2007) Molecular cloning and function analysis of the *stay green* gene in rice. Plant J **52**: 197-209.

John I, Drake R, Farrell A, Cooper W, Lee P, Horton P, Grierson D (1995) Delayed leaf senescence in ethylene deficient ACC-oxidase antisense tomato plants: molecular and physiological analysis. Plant J **7**: 483-490

Johnson-Flanagan A, Thiagarajah M (1990) Degreening in canola (*Brassica napus*, cv westar) embryos under optimum conditions. J Plant Physiol **136**: 180-186

Jordan BR (2002) Molecular responses of plant cells to UV-B stress. Funct Plant Biol **29**: 909–916.

Kao CH, Yang SF (1983) Role of ethylene in the senescence of detached rice leaves. Plant Physiol **73**: 881-885.

Kato M, Ikoma Y, Matsumoto H, Sugiura M, Hyodo H, Yano M (2004) Accumulation of carotenoids and expression of the carotenoid biosynthetic genes during maturation in citrus fruit. Plant Physiol **134**: 1-14

Kim HS, Yu Y, Snesrud EC, Moy LP, Linford LD, Haas BJ, Nierman WC Quackenbush J (2005) Transcriptional divergence of the duplicated oxidative stress-responsive genes in the Arabidopsis genome. Plant J **41**: 212-220

Kimura M, Yamamoto YY, Seki M, Sakurai T, Sato M, Abe T, Yoshida S, Manabe K, Shinozaki K, Matsui M (2003) Identification of Arabidopsis genes regulated by high light-stress using cDNA microarray. Photochemistry and Photobiology **77**: 226-233

Kuehn GD and Phillips GC (2005) Role of polyamines in apoptosis and other recent advances in plant polyamines. Crit Rev Sci **24**: 123-130

Kusaba M, Ito H, Morita R, Iida S, Sato Y, Fujimoto M, Kawasaki S, Tanaka R, Hirochika H, Nishimura M, Tanaka A (2007) Rice NON-YELLOW COLORING1 is involved in light-harvesting complex II and grana degradation during leaf senescence. Plant Cell **19**: 1362-1375

Laitalainen T, Pitkänen J, Hynninen P (1990) Diastereoselective 13^2-hydroxylation of chlorophyll a with SeO_2. In Abstracts of the 8^{th} International IUPAC Conference on Organic Synthesis. IUPAC, Helsinki, pp 246

Lam, H-M, Hsieh M-H, Coruzzi G (1998) Reciprocal regulation of distinct asparagine synthetase genes by light and metabolites in *Arabidopsis thaliana*. Plant J **16**: 345-353

Lee GJ, Roseman AM, Saibil HR, Vierling E (1997) A small heat shock protein stably binds heat-denatured model substrates and can maintain a substrate in a folding-competent state. EMBO J **16**: 659–671

Li XP, Gan R, Li PL, Ma YY, Zhang LW, Zhang R, Wang Y, Wang NN (2006) Identification and functional characterization of a leucine-rich repeat receptor-like kinase gene that is involved in regulation of soybean leaf senescence. Plant Mol Biol **61**: 829-844

Luquez VM, Guiamét JJ (2002) The stay green mutations d1 and d2 increase water stress susceptibility in soybeans. J Exp Bot **376**: 1421-1428

Mahalingam R, Shah N. Scrymgeour A, Fedoroff N (2005) Temporal evolution of the Arabidopsis oxidative stress response. Plant Mol Biol **57**: 709-730

Mínguez-Mosquera MI, Garrido-Fernández J (1989) Chlorophyll and carotenoid presence in olive fruit (*Olea europaea* L.). J Agric Food Chem **37**: 1-7

Mínguez-Mosquera MI, Gandul-Rojas B, Montaño-Asquerino A, Garrido-Fernández J (1991) Determination of chlorophylls and carotenoids by HPLC during olive lactic fermentation. J Chromatog **585**: 259-266

Mínguez-Mosquera MI, Gallardo-Guerrero L, Gandul-Rojas B (1993) Characterization and separation of oxidized derivatives of pheophorbide a and b by thin-layer and high-performance liquid chromatography. J Chromatog **633**: 295-299

Mínguez-Mosquera MI, Gandul-Rojas B, Gallardo-Guerrero L (1994) Measurement of chlorophyllase activity in olive fruit (*Olea europaea*). J Biochem **116**: 263-268

Mitler R, Vanderauwera S, Gollery M, Breusegem FV (2004) Reactive oxygen gene network of plants. Trends Plant Sci **9**:490-498

Montané MH, Kloppstech K (2000) The family of light-harvesting-related proteins (LHCs, ELIPs, HLIPs): was the harvesting of life their primary function? Gene **258**: 1-8

Neta-Sharir I, Isaacson T, Lurie S, Weiss D (2005) Dual role for tomato heat shock protein 21: protecting photosystem II from oxidative stress and promoting color changes during fruit maturation. Plant Cell **17**: 1829-1838

Niyogi KK (1999) Photoprotection revisited. Annu Rev Plant Physiol Plant Mol Biol **50**: 333-359

Oh MH, Moon YH, Lee CH (2003) Increased stability of LHCII by aggregate formation during dark-induced leaf senescence in the *Arabidopsis* mutant, *ore 10*. Plant Cell Physiol **44**: 1368-1377

Oh MH, Kim JH, Moon YH, Lee CH (2004) Defects in a proteolytic step of light-harvesting complex II in an *Arabidopsis* stay-green mutant, *ore10*, during dark-induced leaf senescence. J Plant Biol **47**: 330337

Park SY, Yu JW, Park JS, Li J, Yoo SC, Lee NY, Lee SK, Jeong SW, Seo HS, Koh HJ, Jeon JS, Park YI, Paek NC (2007) The senescence-induced staygreen protein regulates chlorophyll degradation. Plant Cell **19**:1649-1664

Rampino P, Spano G, Pataleo S, Mita G, Napier JA, Di Fonzo N, Shewry PR, Perrotta C (2006) Molecular analysis of a durum wheat 'stay green' mutant: Expression pattern of photosynthesis-related genes. J Cereal Sci **43**: 160-168

Ren G, An K, Liao Y, Zhou X, Cao Y, Zhao H, Ge X Kuai B (2007) Identification of a novel chloroplast protein AtNYE1 regulating chlorophyll degradation during leaf senescence in Arabidopsis. Plant Physiol **144**: 1429-1441

Rizhsky L, Davletova S, Liang H, Mittler R (2004) The zinc-finger protein Zat12 is required for cytosolic ascorbate peroxidase 1 expression during oxidative stress in *Arabidopsis*. J Biol Chem **279**: 11736-11743

Roca M, James J, Pruzinska A, Hortensteiner S, Thomas H, Ougham H (2004) Analysis of the chlorophyll catabolism pathway in leaves of an introgression senescence mutant of *Lolium temulentum*. Phytochem **65**: 1231-1238

Roca M, Mínguez-Mosquera MI (2006) Chlorophyll catabolism pathway in fruits of *Capsicum annuum* (L.): Stay-green versus red fruits. J Agric Food Chem **54**: 4035-40

Rodrigo MJ, Marcos J, Alférez F, Mallent M.D, Zacarías L (2003) Characterization of Pinalate, a novel C*itrus sinensis* mutant with a fruit-specific alteration that results in yellow pigmentation and decreased ABA content. J Exp Bot **54**: 727-738

Rodrigo MJ, Marcos JF, Zacarías L (2004) Biochemical and molecular analysis of carotenoid biosynthesis in flavedo of orange (*Citrus sinensis* L.) during fruit development and maturation. J Agric Food Chem **52**: 6724-6731

Ronning CM, Bouwkamp JC, Solomos T (1991) Observations on the senescence of a mutant non-yellowing genotype of *Phaseolus vulgaris* L. J. Exp. Bot **235**: 235-241

Rose JKC, Bashir S, Giovannoni JJ, Jahn MM, Saravanan RS (2004) Tackling the plant proteome: Practical approaches, hurdles and experimental tools. Plant J **39**: 715-733

Rossel JB, Wilson IW, Pogson BJ (2002) Global changes in gene expression in response to high light in Arabidopsis. Plant Physiol **130**: 1109-1120

Rossini S, Casazza AP, Engelmann EC, Havaux M, Jennings RC, Soave C (2006) Suppression of both ELIP1 and ELIP2 in Arabidopsis does not affect tolerance to photoinhibition and photooxidative stress. Plant Physiol **141**: 1264-1273

Sambrook J, Fitsh EF, Maniatis T (1989) Molecular cloning: A laboratory manual, Cold Spring Harbor Laboratory Press, Cold Spring Harbor, NY

Saravanan RS, Rose JKC (2004) A critical evaluation of sample extraction techniques for enhanced proteomic analysis of recalcitrant plant tissues. Proteomics 4: 2522-2532

Sato Y, Morita R, Nishimura M, Yamaguchi H, Kusaba M (2007) Mendel's green cotyledon gene encodes a positive regulator of the chlorophyll-degrading pathway. Proc Natl Acad Sci USA **104**: 14169-14174.

Smart CM, Scofield SR, Bevan MW, Dyer TA (1991) Delayed leaf senescence in tobacco plants transformed with *tmr*, a gene for cytokinin production in *Agrobacterium*. Plant Cell **3**: 647-656

Smith JHC Benítez A (1955) Chlorophylls. In Modern Methods of Plant Analysis, K Paech, MM Tracey, eds. Springer, Berlin, pp 142-196

Spano G, Di Fonzo N, Perrotta C, Platani C, Ronga G, Lawlor DW, Napier JA, Shewry PR (2003) Physiological characterisation of 'stay green' mutants in durum wheat. J Exp Bot **386**: 1415-1420

Sun W, van Montagu M, Verbruggen, N (2002) Small heat shock proteins and stress tolerance in plants. Biochim Biophys Act **1577**: 1–9

Takahama U, Oniki T (1992) Regulation of peroxidase-dependent oxidation of phenolics in the apoplast of spinach leaves by ascorbate. Plant Cell Physiol **33**: 379-387.

Tanaka R, Oster, U, Kruse, E, Rudiger, W, Grimm, B (1999) Reduced activity of geranylgeranyl reductase leads to loss of chlorophyll and tocopherol and to partially geranylgeranylated chlorophyll in transgenic tobacco plants expressing antisense RNA for geranylgeranyl reductase. Plant Physiol **120**: 695-704

Terpstra W, Lambers J (1983) Interactions between chlorophyllase, chlorophyll a, plants lipids and Mg^{2+}. Biochim Biophys Act **746**: 23-31

Thomas H (1987) *Sid*: a Mendelian locus controlling thylakoid membrane disassembly in senescing leaves of *Festuca pratensis*. Theor Appl Gen **73**: 551-555

Thomas H, Ougham H, Canter P, Donnison I (2002) What stay-geen mutants tell us about nitrogen remobilization in leaf senescence. J exp bot **53**:801-808

Thomas H, Schellenberg M, Vicentini F, Matile P (1996) Gregor Mendel's green and yellow pea seeds. Bot Act **109**: 3-4

Thomas H, Howarth CJ (2000) Five ways to stay green. J Exp Bot **51**: 329-337

Tosti N, Pasqualini S, Borgogni A, Ederli L, Falistocco E, Crispi S, Paolocci F (2006) Gene expression profiles of O_3-treated *Arabidopsis* plants. Plant Cell Environ **29**: 1686-1702

Trebitsh T, Goldschmidt EE, Riov J (1993) Ethylene induces de novo synthesis of chlorophyllase, a chlorophyll degrading enzyme, in Citrus fruit peel. Proc Natl Acad Sci USA **90**: 9441-9445

Vicentini F, Hörtensteiner S, Schellenberg M, Thomas H, Matile, P (1995) Chlorophyll breakdown in senescent leaves: identification of the biochemical lesion in a stay-green genotype of *Festuca pratensis* Huds. New Phytol **129**: 247-252

Watanabe T, Hongu A, Honda K, Nakazato M, Konno M, Saithoh S. (1984) Preparation of chlorophylls and pheophytins by isocratic liquid chromatography. Annals Chem **56**: 251-256

Woo HR, Chung KM, Park JH, Oh SA, Ahn T, Hong SH, Jang SK, Nam HG (2001) ORE9, an F-box protein that regulates leaf senescence in Arabidopsis. Plant Cell **13**: 1779-1790

Wong CE, Li Y, Labbe A, Guevara D, Nuin P, Whitty B, Diaz C, Golding GB, Gray GR, Weretilnyk EA Griffith M, Moffatt CA (2006) Transcriptional profiling implicates novel interactions between abiotic stress and hormonal responses in Thellungiella, a close relative of Arabidopsis. Plant Physiol **140**: 1437-1450

Yamamoto A, Bhuiyan NMH, Watidee R, Tanaka Y, Esaka M, Oba K, Jagendorf AT Takabe T (2005) Suppressed expression of the apoplastic ascorbate oxidase gene increases salt tolerance in tobacco and *Arabidopsis* plants. J Exp Bot **56**: 1785-1796

Young R. Jahn O (1972) Ethylene- induced carotenoid accumulation in citrus fruit rinds. J Amer Soc Hort Sci **97**: 258-261

Zhao J, Williams, CC, Last RL (1998) Induction of Arabidopsis tryptophan pathway enzymes and camalexin by amino acid starvation, oxidative stress, and an abiotic elicitor. Plant Cell **10**: 359-370

FIGURE LEGENDS

Figure 1. Scheme of the Chl degradative pathway in higher plants. CLH, chlorophyllase; MCS, metal chelating substance; PaO, pheophorbide a oxygenase; RCC, red chlorophyll catabolite; RCCR, red chlorophyll catabolite reductase; pFCC, primary fluorescent chlorophyll catabolite; NCCs, non-fluorescent chlorophyll catabolites.

Figure 2. External (**A**) and internal (**B**) appearance of WT and *navel negra* (*nan*) fruits at a full-ripe stage (275 DPA) and quantification of total chlorophylls (**C**) and carotenoids (**D**) in the flavedo of *Citrus sinensis* cvs Washington Navel (WT, open circles) and *nan* (filled circles) during fruit ripening. Data are means ± S.E, n = 3. Error bars smaller than symbol size are not visible. MG, mature green stage (180 DPA); B, breaker stage (224 DPA); R, ripe stage (248 DPA).

Figure 3. Expression analysis by real time RT-PCR of transcripts in the flavedo of WT (open circles) and the *nan* mutant (filled circles) of (**A**) *PSY* (phytoene synthase), (**B**) *CHL P* (geranylgeranyl reductase), (**C**) *PaO* (pheophorbide a oxygenase), and (**D**) *RCCR* (red chlorophyll catabolite reductase) during fruit growth and ripening. An expression value of 1 was arbitrarily assigned to the 120 DPA sample of WT. MG, mature green stage (180 DPA); B, breaker stage (224 DPA); R, ripe stage (248 DPA). Data are means ± S.E, n = 3. Error bars smaller than symbol size are not visible.

Figure 4. Effects of ethylene treatments on both total pigment composition (**A)** and changes in mRNA abundance (**B**) in the flavedo of WT (open columns) and *nan* (filled columns). Fruits were treated with 10 µl L^{-1} ethylene in controlled atmosphere postharvest chambers at 20 ºC for 72 h. Pigment content was expressed as the absolute increment between control and treated samples. Transcript abundance of *PSY* (phytoene synthase), *CHL P* (geranylgeranyl reductase), *CHL* (chlorophyllase) and *PaO* (pheophorbide a oxygenase) was determined by real time RT-PCR. Expression ratio between treated and untreated fruits was calculated and $\log_2$-transformed. All data are means ± S.E, n = 3.

Figure 5. Relative gene expression in the flavedo of WT and *nan* of (**A**) stay green, (**B**) secretory peroxidase and (**C**) cysteine proteinase transcripts determined by real time RT-PCR. MG, mature green stage (180 DPA); B, breaker stage (224 DPA); R, ripe stage (248 DPA). Log_2-transformed mean ratios of *nan*/WT expression ± SE are presented, n = 3. GenBank accession numbers of the ESTs are indicated in parentheses.

Figure 6. Immunoblot analysis of RuBisCO expression in flavedo of WT and *nan*. Bands corresponding to the large subunit (LSU) and small subunit (SSU) are highlighted. MG, Mature green stage (180 DPA); B, Breaker stage (224 DPA); R, Ripe stage (248 DPA). Molecular weight markers are indicated.

Figure 7. Transcript levels of the *early light-inducible protein* (*ELIP)* gene during fruit growth and ripening in the flavedo of WT (open circles) and *nan* (filled circles). Analyses were performed by real time RT-PCR and an expression value of 1 was arbitrarily assigned to the 120 DPA sample of WT. MG, mature green stage (180 DPA); B, breaker stage (224 DPA); R, ripe stage (248 DPA). Data are means ± S.E, n = 3. Error bars smaller than symbol size are not visible.

Table I. Chlorophylls and derivatives and chlorophyllase activity in the flavedo of WT citrus and the *nan* stay green mutant at mature green (180 DPA), breaker (224 DPA) and ripe (248 DPA) stages.

	Mature Green Stage		Breaker Stage		Ripe Stage	
	WT	*nan*	WT	*nan*	WT	*nan*
Pigments (µg g^{-1} FW)						
Chlorophyll *a*	105.35 ± 8.25	120.32 ± 5.21	2.64 ± 0.03	100.65 ± 2.64	1.05 ± 0.01	105.34 ± 9.65
OH-Chlorophyll *a*	0.52 ± 0.02	1.42 ± 0.11	N.D.	0.99 ± 0.02	N.D	5.21 ± 0.02
Pheophytin *a*	2.01 ± 0.01	1.75 ± 0.05	0.09 ± 0.01	0.68 ± 0.06	0.40 ± 0.04	0.65 ± 0.11
Chlorophyll *b*	23.51 ± 1.57	16.57 ± 0.08	0.83 ± 0.01	21.36 ± 1.12	N.D.	9.65 ± 0.54
OH-chlorophyll *b*	N.D.	N.D.	N.D.	N.D.	N.D.	1.06 ± 0.09
Total chlorophylls	131.39 ± 8.64	140.24 ± 15.36	3.56 ± 0.46	123.68 ± 3.21	0.07 ± 0.01	120.85 ± 8.24
Chlorophyllide a	N.D.	N.D.	N.D.	N.D.	N.D.	N.D.
Pheophorbide a	N.D.	N.D.	N.D.	N.D.	N.D.	N.D.
Chlorophyllase activity (µmol h^{-1} g^{-1} FW)	4.5 ± 0.3	4.4 ± 0.3	2.4 ± 0.1	2.1 ± 0.1	1.8 ± 0.2	2.4± 0.2

N.D.: not detected. Data are means ± S.E, n = 3.

Table II. Genes showing significant expression changes in the flavedo of WT and the *nan* stay green mutant at all three stages studied: mature green (180 DPA), breaker (224 DPA) and ripe (248 DPA) stages. Differences in gene expression of at least 2-fold (P-value ≤ 0.001) in each of 3 replicates were considered to be statistically significant.

Citrus EST Accession number	tBLASTx best hit	[a]Identities	Arabidopsis ortholog	Mature Green Log_2 ratio[b]	Breaker Log_2 ratio[b]	Ripe Log_2 ratio[b]
CX308230	Stay green protein [*Solanum lycopersicum*]	86%	At4g22920	-1.97 ± 0.11	-1.71 ± 0.12	-1.67 ± 0.11
CX305230	Miraculin-like protein 2 [*Citrus jambhiri*]	96%	At1g17860	1.08 ± 0.17	-1.72 ± 0.18	-1.30 ± 0.17
CX308252	Secretory peroxidase [*Nicotiana tabacum*]	89%	At4g21960	2.19 ± 0.16	-1.02 ± 0.18	-2.76 ± 0.16
CX302192	Guanyl-nucleotide exchange factor [*Arabidopsis thaliana*]	71%	At1g01960	1.99 0.14	-2.14 ± 0.15	-1.02 ± 0.14
CX305503	Cysteine proteinase [*Citrus sinensis*]	100%	At4g32940	-1.05 ± 0.20	1.42 ± 0.21	1.52 ± 0.20

[a] Identities at the amino acid level. [b] Induction fold are expressed as log-transformed mean ratios of *nan* /WT expression.

Table III. Examples of genes showing different expression levels in the flavedo of WT orange or the *nan* stay green mutant at mature green stage (180 DPA), as determined with a citrus microarray, highlighting those associated with oxidative stress, chloroplast function or senescence. References describing such an association for the Arabidopsis ortholog of the citrus gene are indicated. Differences in gene expression of at least 2-fold (P-value ≤ 0.001) in each of 3 replicates were considered to be statistically significant.

Mature Green						
Functional Class	Best BLAST hit	Higher expression		Citrus EST accession	Arabidopsis ortholog	Related References
		WT	*nan*			
Primary metabolism	plastidic glucose 6-phosphate dehydrogenase		●	CX293894	At5g13110	Debnam et al. (2004)
	chloroplastic aspartate aminotransferase		●	CX294238	At2g22250	de la Torre et al. (2006)
	asparagine synthetase	●		CX306022	At3g47340	Lam et al. (1998)
Photosynthesis, light signaling	RPT2		●	CX300991	At2g30520	Inada et al. (2004)
	NADH protochlorophyllide oxidoreductase	●		CX289541	At5g54190	Rossel et al. (2002)
	PS I subunit L	●		CX287010	At4g12800	Kimura et al. (2003)
	PS I subunit E	●		CX300489	At2g20260	
	putative PS I subunit	●		CX299745	At4g02770	Kimura et al. (2003)
	chlorophyll a/b binding protein 3	●		CX287196	At1g29910	Kimura et al. (2003)
	PS II type I chlorophyll a/b binding protein	●		CX300355	At2g34430	Kimura et al. (2003)
	Lhcb2 protein	●		CX300473	At3g27690	Kimura et al. (2003)
	Lhcb6 protein	●		CX300344	At1g15820	Rossel et al. (2002)
	Lhca2	●		CX300483	At3g61470	Kimura et al. (2003)
	RuBisCO subunit binding protein (chaperonin)	●		CX300392	At2g28000	Tosti et al. (2006)
ROS, redox	secretory peroxidase		●	CX308252	At4g21960	
	FAD-linked oxidoreductase	●		CX292465	At5g44380	Kim et al. (2005)
	metallothionein protein	●		CX303735	At3g15353	Guo et al. (2004)
Phenylpropanoids	phenylalanine-ammonia lyase		●	CX308098	At2g37040	Rossel et al. (2002)
	chalcone synthase		●	CX308007	At5g13930	Rossel et al. (2002)
	flavonol 3'-O-methyltransferase		●	CX308025	At5g54160	Kimura et al. (2003)
	coumarate 3-hydroxylase		●	CX290216	At2g40890	
Polyamines	SAM decarboxylase		●	CX308026	At3g02470	Guo et al. (2004)
Protein stability	chloroplastic heat shock protein	●		CX292078	At4g27670	
	HSP20	●		CX309295	At2g29500	Kim et al. (2005)
	heat shock protein		●	CX294165	At3g52490	
Defense	chitinase	●		CX292066	At3g54420	
Miscellaneous	β-amylase		●	CX291892	At3g23920	Rossel et al. (2002)
	UVI-1 homolog		●	CX301008	At1g19020	Gadjev et al. (2006)
	glycine rich RNA binding protein	●		CX287915	At3g26740	Kimura et al. (2003)

Table IV. Examples of genes showing different expression levels in the flavedo of WT orange or the *nan* stay green mutant at the ripe stage (248 DPA), as determined with a citrus microarray, highlighting those associated with oxidative stress, chloroplast function or senescence. References describing such an association for the Arabidopsis ortholog of the citrus gene are indicated. Differences in gene expression of at least 2-fold (P-value ≤ 0.001) in each of 3 replicates were considered to be statistically significant.

Ripe						
Functional Class	Best BLAST hit	Higher expression WT	Higher expression *nan*	Citrus EST accession	Arabidopsis ortholog	Related References
Primary metabolism	tryptophan synthase		●	CX291092	At5g54810	Zhao et al. (1998)
Photosynthesis, light signaling	Lhcb2 protein		●	CX200280	At2g05100	Kimura et al. (2003)
ROS, redox	cytochrome bf6 complex subunit		●	CX37372	At2g26500	Kimura et al. (2003)
	GST1		●	CX301042	At2g30860	Rossel et al. (2002)
	GST6	●		CX288839	At2g47730	Rossel et al. (2002)
	peroxidase	●		CX308204	At4g21960	Wong et al. (2006)
	ascorbate oxidase	●		CX289525	At5g21100	Yamamoto et al. (2005)
Phenylpropanoids	isoflavone reductase-like		●	CX308502	At4g39230	
	flavonol 3'-O-methyltransferase		●	CX289068	At5g54160	Kimura et al. (2003)
Polyamines	SAM decarboxylase		●	CX289919	At3g25570	Guo et al. (2004)
Isoprenoids, carotenoids	geranylgeranyl diphosphate synthase		●	CX290062	At3g14510	
Salicylic acid	SAM-dependent methyltransferase		●	CX308455	At3g11480	Chen et al. (2003)
Jasmonic acid	Lipoxygenase (LOX3)		●	CX288539	At1g17420	Mahalingam et al. (2005)
Ethylene	ACC oxidase		●	CX292573	At1g05010	Gadjev et al. (2006)
Defense	chitinase	●		CX291879	At3g12500	Bray (2002)
Miscellaneous	miraculin	●		CX306063	At1g17860	Rizhsky et al. (2004)
	cysteine protease (SAG12)		●	CX287658	At5g45890	Guo et al. (2004)
	glycosyltransferase		●	CX288595	At3g11340	Gadjev et al. (2006)
	glutamate decarboxylase		●	CX288553	At5g17330	
	vacuolar processing enzyme		●	CX287419	At4g32940	Gepstein et al. (2003)

Table V. Relative changes in the abundance of 11 protein spots in the flavedo of WT and the *nan* mutant at mature green (180 DPA), breaker (224 DPA) and ripe (248 DPA) stages, as determined using 2D-DIGE. Differentially expressed spots were defined as those with a volume ratio above or below the 2 S.D. threshold based on the normalized model curve of the spot volume ratio data set. Protein annotation was performed after a search in the NCBI non-redundant Green Plant database. The accession numbers and corresponding protein scores are listed. Data are the means ± S.E. (n = 4) of the normalized spot volume *nan*/WT ratio. Arrows (→) indicate no significant changes in relative protein abundance.

Spot	Accession number	Best Hit	Protein Score	Fold change		
				Mature Green	Breaker	Ripe
1	gi|54292100	manganese superoxide dismutase (*Camellia sinensis*)	103	2 ± 0.05	2 ± 0.2	→
2	gi|14158	heat shock protein 21 (*Petunia x hybrida*)	101	-5.5 ± 2.1	-3.0 ± 0.6	-2.7 ± 0.6
3	gi|30039180	copper chaperone (*Solanum lycopersicum*)	53	4.8 ± 0.5	→	→
4	gi|2274917	Cu/Zn superoxide dismutase (*Citrus sinensis*)	61	5 ± 0.3	→	7.1 ± 0.7
5	gi|6911142	glycine-rich RNA binding protein 1 (*Catharanthus roseus*)*]*	42	-7.4 ± 0.1	→	→
6	gi|4206520	ribulose 1,5-bisphosphate carboxylase (*Severinia buxifolia*)	851	→	-2.2 ± 0.1	-2.7 ± 0.1
7	gi|4206520	ribulose 1,5-bisphosphate carboxylase (*Severinia buxifolia*)	711	→	-2.3 ± 0.1	-3.4 ± 0.1
8	gi|11596188	lectin-related protein precursor (*Citrus x paradisi*)	329	→	-3.8 ± 0.6	-3.2 ± 1.0
9	gi|7447856	early light-inducible protein precursor (*Glycine max*)	56	→	6.6 ± 0.7	14 ± 3.7
10	gi|8778393	F16A14.17 (*Arabidopsis thaliana*)	47	→	2.8 ± 0.6	→
11	gi|30575572	HSP19 class I (*Citrus x paradisi*)	168	→	→	2.8 ± 0.02

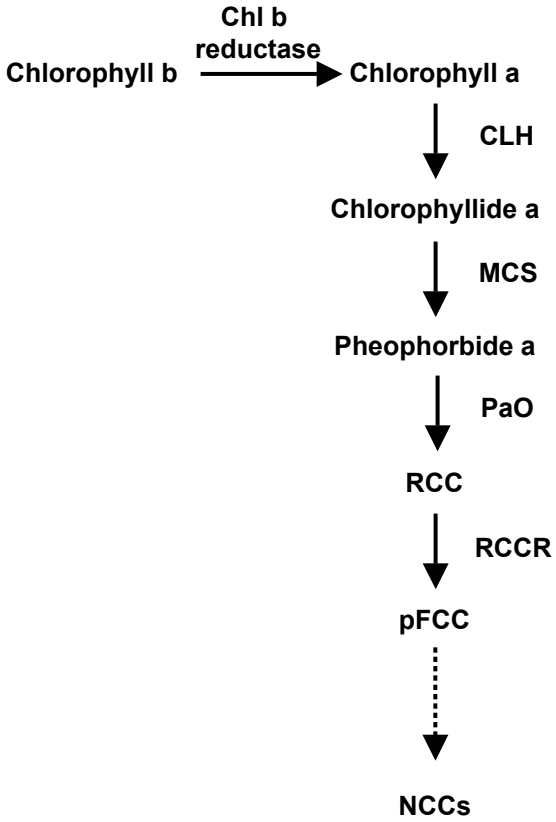

Figure 1. Scheme of the Chl degradative pathway in higher plants. CLH, chlorophyllase; MCS, metal chelating substance; PaO, pheophorbide a oxygenase; RCC, red chlorophyll catabolite; RCCR, red chlorophyll catabolite reductase; pFCC, primary fluorescent chlorophyll catabolite; NCCs, non-fluorescent chlorophyll catabolites.

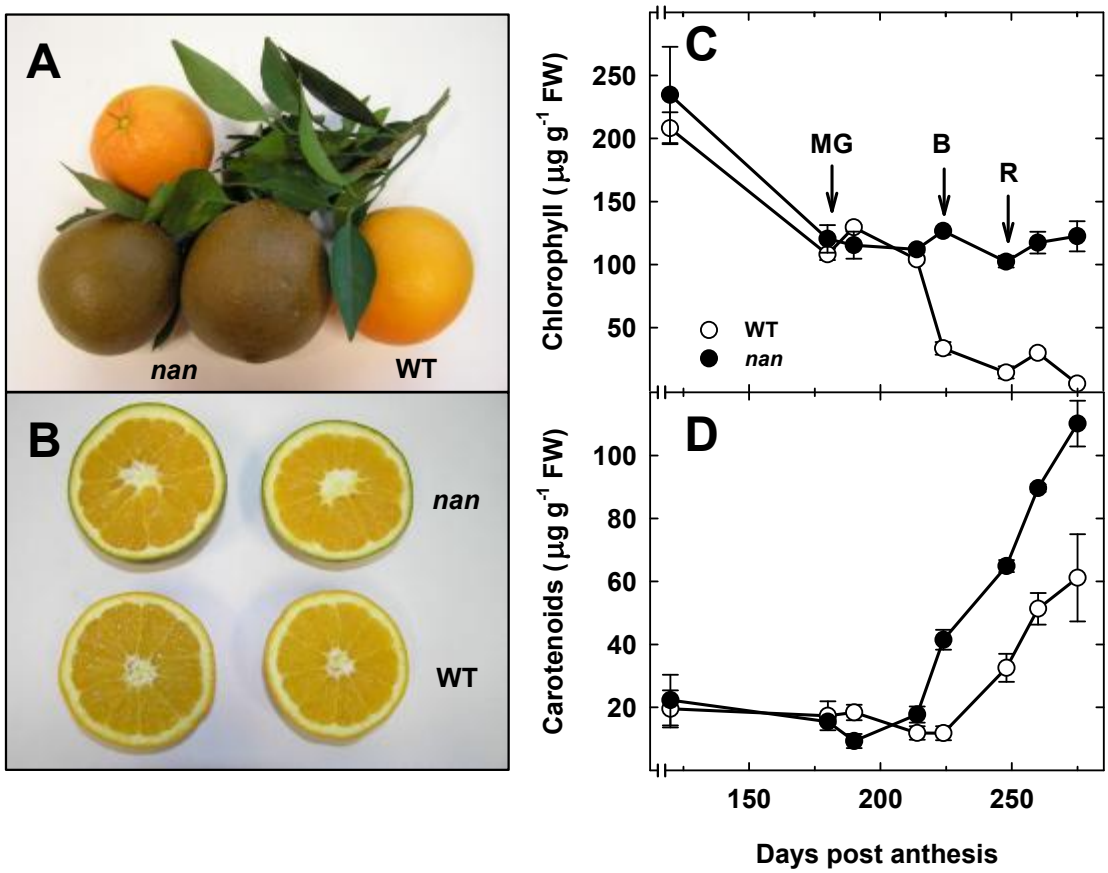

Figure 2. External (**A**) and internal (**B**) appearance of WT and *navel negra* (*nan*) fruits at a full-ripe stage (275 DPA) and quantification of total chlorophylls (**C**) and carotenoids (**D**) in the flavedo of *Citrus sinensis* cvs Washington Navel (WT, open circles) and *nan* (filled circles) during fruit ripening. Data are means ± S.E, n = 3. Error bars smaller than symbol size are not visible. MG, mature green stage (180 DPA); B, breaker stage (224 DPA); R, ripe stage (248 DPA).

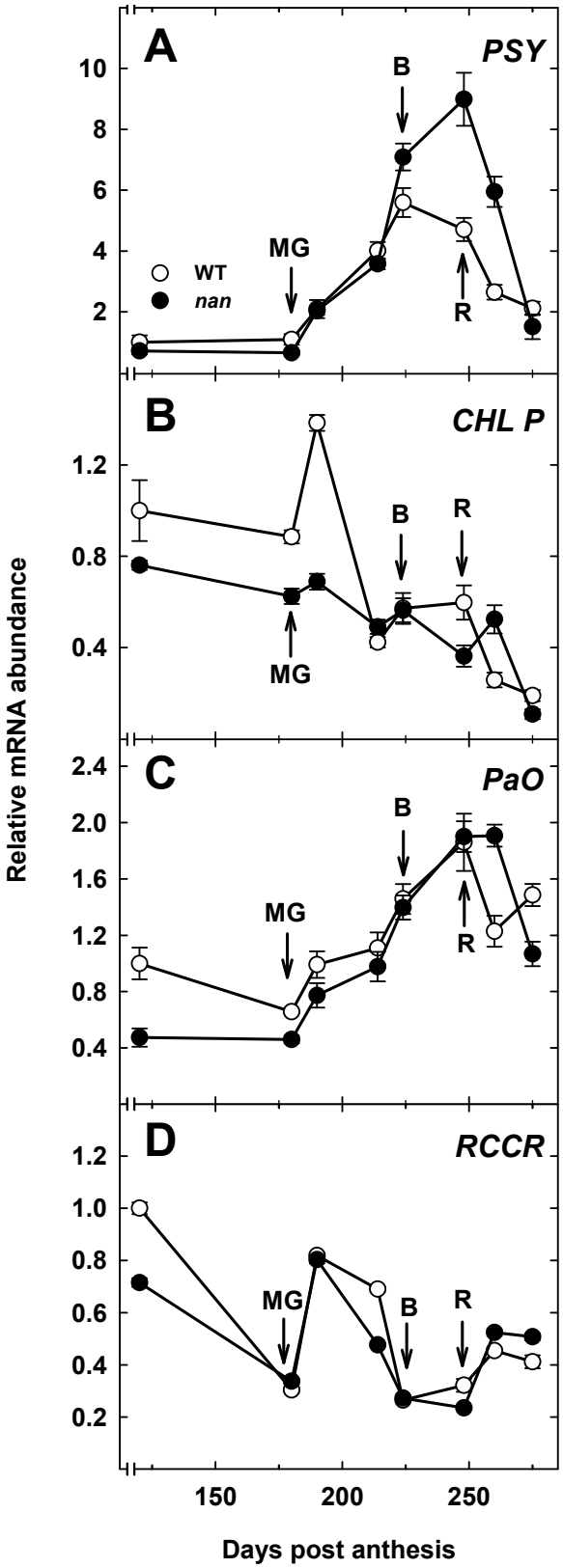

Figure 3. Expression analysis by real time RT-PCR of transcripts in the flavedo of WT (open circles) and the *nan* mutant (filled circles) of (**A**) *PSY* (phytoene synthase), (**B**) *CHL P* (geranylgeranyl reductase), (**C**) *PaO* (pheophorbide a oxygenase), and (**D**) *RCCR* (red chlorophyll catabolite reductase) during fruit growth and ripening. An expression value of 1 was arbitrarily assigned to the 120 DPA sample of WT. MG, mature green stage (180 DPA); B, breaker stage (224 DPA); R, ripe stage (248 DPA). Data are means ± S.E, n = 3. Error bars smaller than symbol size are not visible.

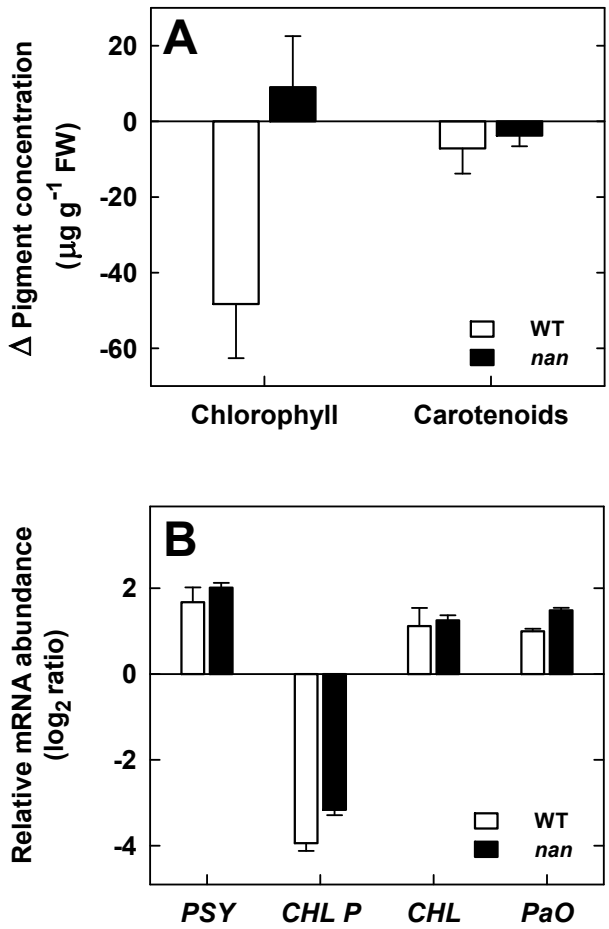

Figure 4. Effects of ethylene treatments on both total pigment composition (**A)** and changes in mRNA abundance (**B**) in the flavedo of WT (open columns) and *nan* (filled columns). Fruits were treated with 10 μl L^{-1} ethylene in controlled atmosphere postharvest chambers at 20 ºC for 72 h. Pigment content was expressed as the absolute increment between control and treated samples. Transcript abundance of *PSY* (phytoene synthase), *CHL P* (geranylgeranyl reductase), *CHL* (chlorophyllase) and *PaO* (pheophorbide a oxygenase) was determined by real time RT-PCR. Expression ratio between treated and untreated fruits was calculated and log_2-transformed. All data are means ± S.E, n = 3.

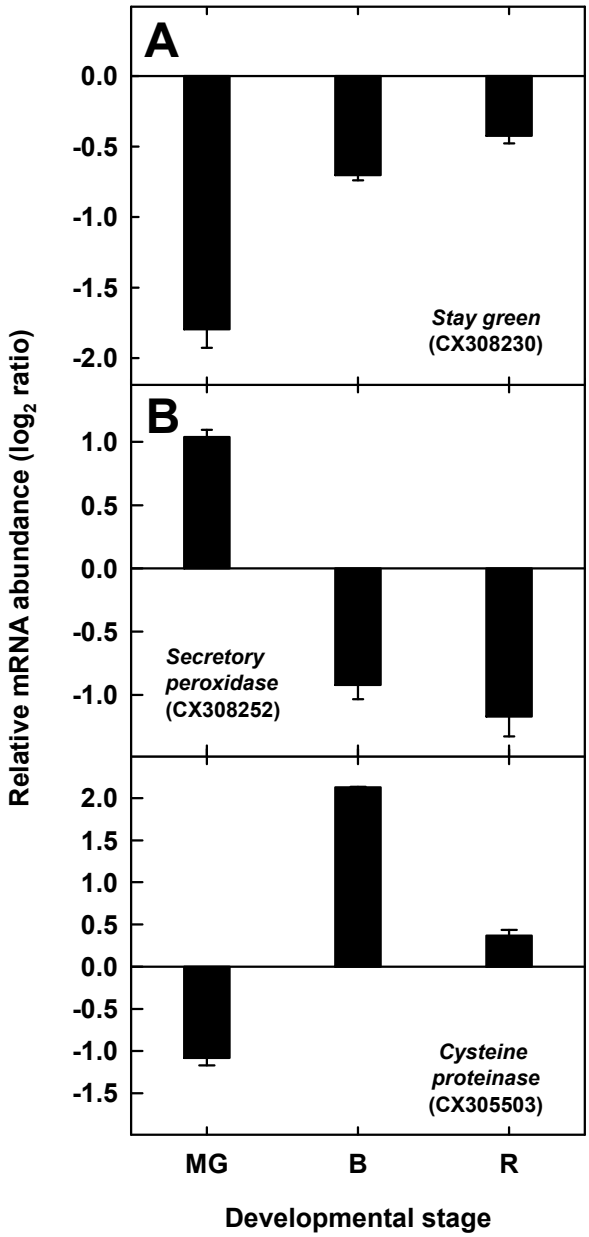

Figure 5. Relative gene expression in the flavedo of WT and *nan* of (**A**) stay green, (**B**) secretory peroxidase and (**C**) cysteine proteinase transcripts determined by real time RT-PCR. MG, mature green stage (180 DPA); B, breaker stage (224 DPA); R, ripe stage (248 DPA). Log_2-transformed mean ratios of *nan*/WT expression ± SE are presented, n = 3. GenBank accession numbers of the ESTs are indicated in parentheses.

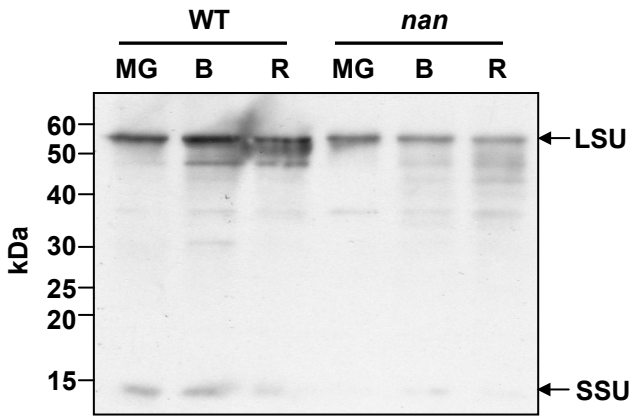

Figure 6. Immunoblot analysis of RuBisCO expression in flavedo of WT and *nan*. Bands corresponding to the large subunit (LSU) and small subunit (SSU) are highlighted. MG, Mature green stage (180 DPA); B, Breaker stage (224 DPA); R, Ripe stage (248 DPA). Molecular weight markers are indicated.

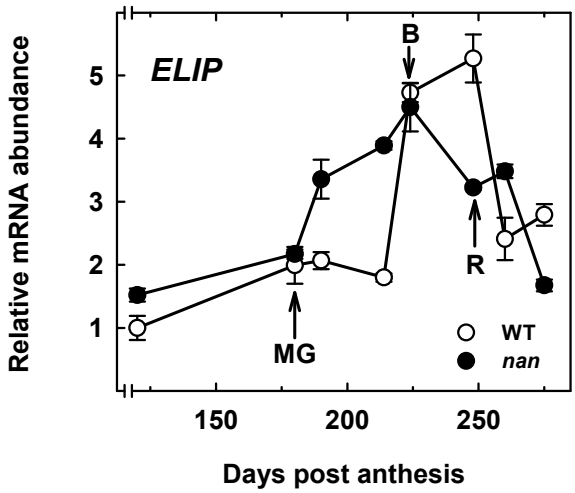

Figure 7. Transcript levels of the *early light-inducible protein* (*ELIP)* gene during fruit growth and ripening in the flavedo of WT (open circles) and *nan* (filled circles). Analyses were performed by real time RT-PCR and an expression value of 1 was arbitrarily assigned to the 120 DPA sample of WT. MG, mature green stage (180 DPA); B, breaker stage (224 DPA); R, ripe stage (248 DPA). Data are means ± S.E, n = 3. Error bars smaller than symbol size are not visible.